Avalanche criticality in externally driven materials

Antoni Planes
(antoniplanes@ub.edu)

Departament de Física de la Matèria Condensada
Universitat de Barcelona

Collaborators

E. Vives, Ll. Mañosa, J. Baró*, D. Soto-Parra** E. Bonnot, P. Castillo-Villa****

Present address: **University of Calgary,* Canada; ** Queen's University*, Belfast;
***IPICyT*, San Luís Potosí, Mexico

Collaborators

E. Vives, Ll. Mañosa, J. Baró*, D. Soto-Parra** E. Bonnot, P. Castillo-Villa****

Present address: **University of Calgary,* Canada; ** Queen's University*, Belfast;
***IPICyT*, San Luís Potosí, Mexico

B. Ludwig , U. Klemradt

E. K. H. Salje

C.Gallardo, J. Romero, J. M. Martín-Olalla

Y. Fan, R. S. Edwards, S. Dixon

R. Romero, M. Stipcich

R. Niemann, S. Fälher

F. J. Pérez-Reche

T. Kakeshita, T. Fukuda

Systems of interest

• Systems that respond to a **slowly driven external field intermittently** with **discrete events** that occur over a **broad range of sizes (avalanches)**.

• This behaviour typically occur in **heterogenous/disordered** systems with **athermal** dynamics.

• Examples:

- Dislocation dynamics
- Plasticity
- Fracture
- Magnetization processes
- Ferroelastic/martensitic transitions

....

- Seismicity

Systems of interest

• Systems that respond to a **slowly driven external field intermittently** with **discrete events** that occur over a **broad range of sizes (avalanches)**.

• This behaviour typically occur in **heterogenous/disordered** systems with **athermal** dynamics.

• Examples:

- Dislocation dynamics
- Plasticity
- **Fracture of porous materials under compression**
- Magnetization processes
- Ferroelastic/**martensitic transitions**

....

- Seismicity

Acoustic emission

AE occurs associated with these externally stimulated processes.

The acoustic waves originates from localized processes that occur at length scales ranging from nano to micrometers that give rise to rapid changes of the internal strain field of the system.

It is typically detected in the frequency range of MHz.

Its detection provides a potentially interesting technique to characterize avalanches and avalanche dynamics.

Detection

Acoustic Emission: Elastic waves originate from the source and propagate through the sample.

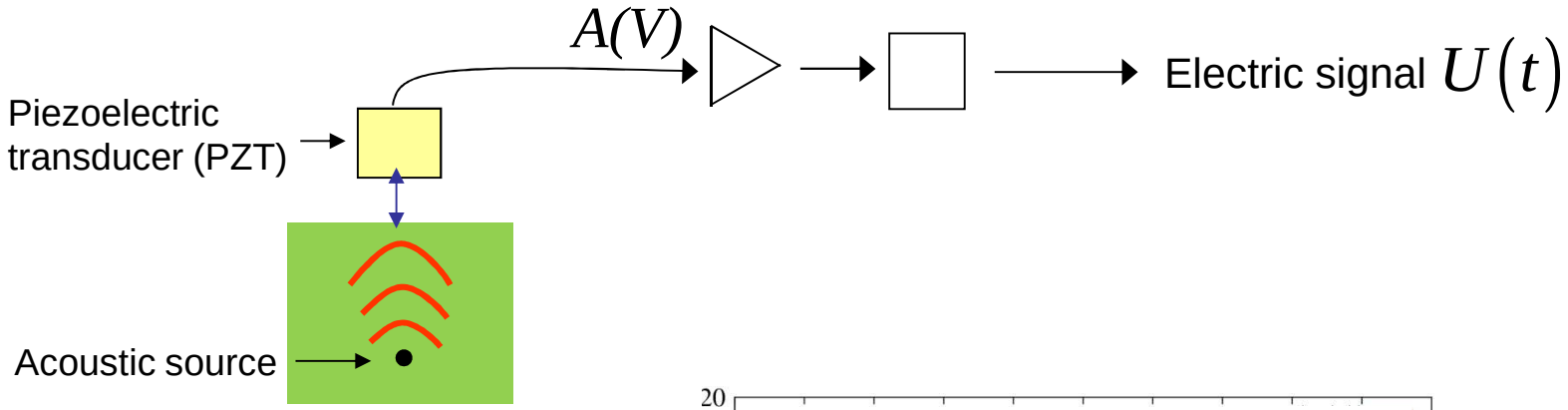

Example of AE signal:

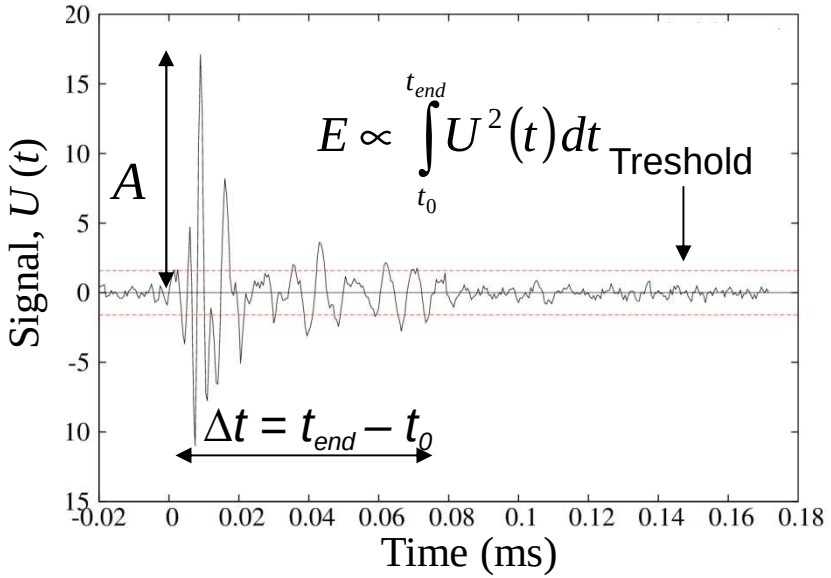

Data analysis

- The AE carries the whole temporal and spatial information of the source mechanism.
- Extracting this information is difficult since the signal $U(t)$ is severely distorted due to the acoustic coupling of the transducer and its frequency response.

Data analysis

- The AE carries the whole temporal and spatial information on the source mechanism.
- Extracting this information is difficult since the signal $U(t)$ is severely distorted due to the acoustic coupling of the transducer and its frequency response.
- Partial information:
  - Pulse counting rate: Acoustic Emission activity

Examples

Martensitic transition in Cu-Zn-Al

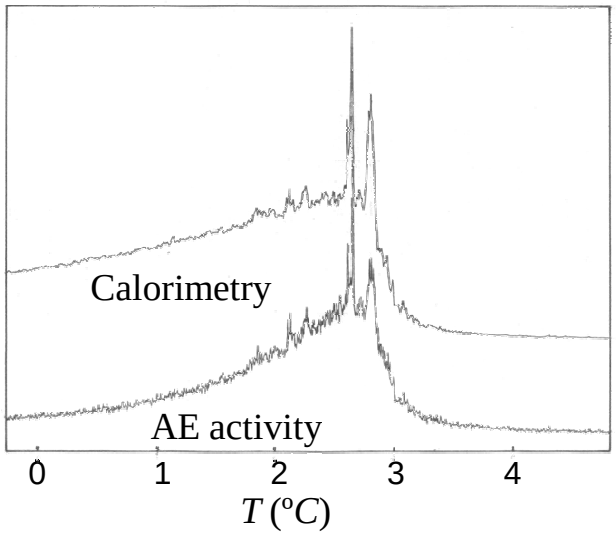

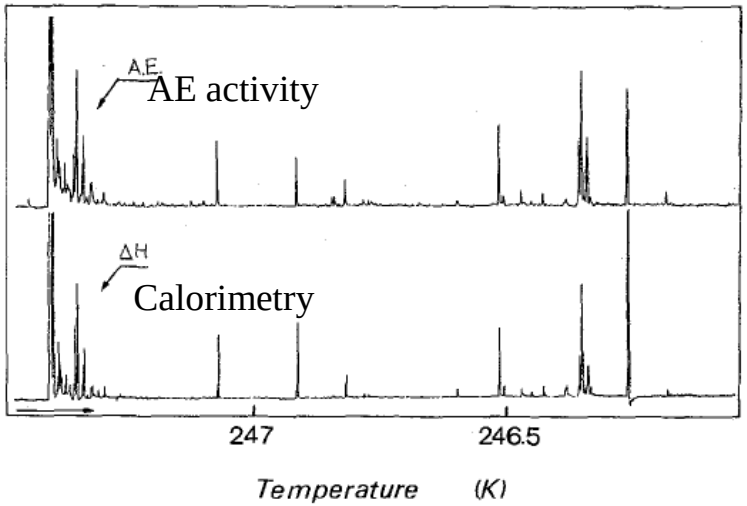

Compression of porous Vycor

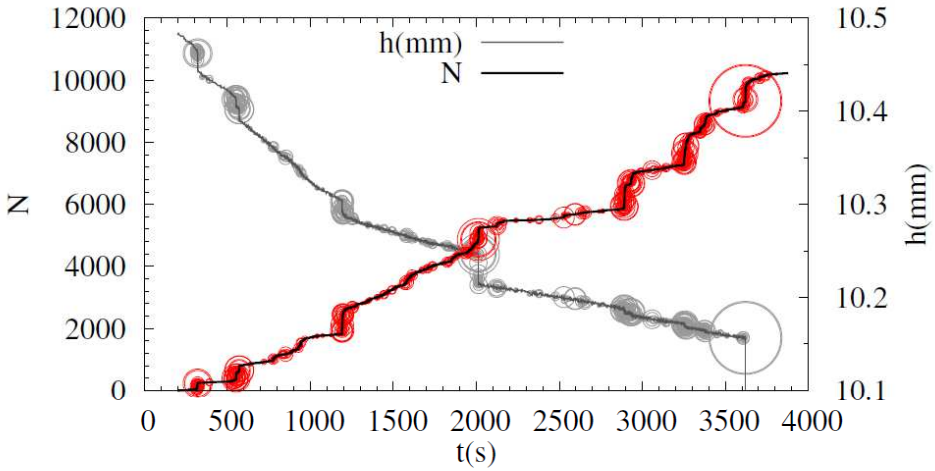

Data analysis

- The AE carries the whole temporal and spatial information on the source mechanism.
- Extracting this information is difficult since the signal $U(t)$ is severely distorted due to the acoustic coupling of the transducer and its frequency response.
- Partial information:
  - Pulse counting rate: Acoustic Emission activity
  - Statistical analysis of the amplitude, energy, duration, waiting-time, ... of the AE signals: provides information related to the **collective** behaviour of the system

Criticality

- Amplitude, energy and duration of AE signals span over a broad range (decades).
- Often the **statistical distribution** of these quantities is **power-law** which is a typical feature of **criticality**, *i.e.*, avalanche dynamics shows **scale invariance**.
- Statistical distribution $\left(Y = A, E, \Delta t\right)$:

$$p(Y) = C_Y \exp\left(-\lambda_Y Y\right) Y^{-\omega}$$

λ_Y: measures the distance to criticality

C_Y: normalization factor

ω: critical exponent (= α, ε, τ corresponding to A, E, Δt)

- Criticality
  - Statistical relation: $\begin{cases} E \sim A^z \\ A \sim \Delta t^x \end{cases}$
  - Scaling relation: $\alpha - 1 = z\left(\varepsilon - 1\right) = x\left(\tau - 1\right)$

Martensitic transition

- A martensitic transformation (ferroelastic) is a diffusionless structural transition from a high symmetry to a lower symmetry crystallographic phase.
- Can be induced by changing temperature and/or stress (conjugated field).
- Shows athermal character and proceeds intermittently as a sequence of jerks (avalanches).
- Produce a complex multiscale domain microstructure.

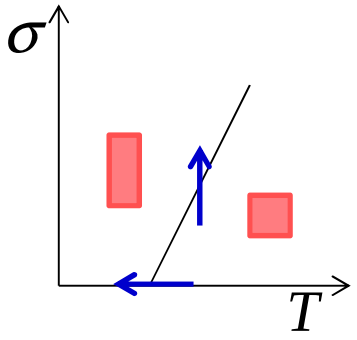

Courtesy of Prof. Michel Morin

Framework

- The intermittent (jerky) character of the transformation is a consequence of dynamical constraints imposed by ***disorder***:
  - Intrinsic disorder: lattice defects, impurities, etc...
  - Self-generated elastic long-range interaction effects.

Framework

- The intermittent (jerky) character of the transformation is a consequence of dynamical constraints imposed by ***disorder***:
  - Intrinsic disorder: lattice defects, impurities, etc...
  - Self-generated: long-range interaction effects.

- The jerks or ***avalanches*** are associated with discontinuities of the strain (*O.P.*) associated with the jumps from one metastable state to another metastable state.

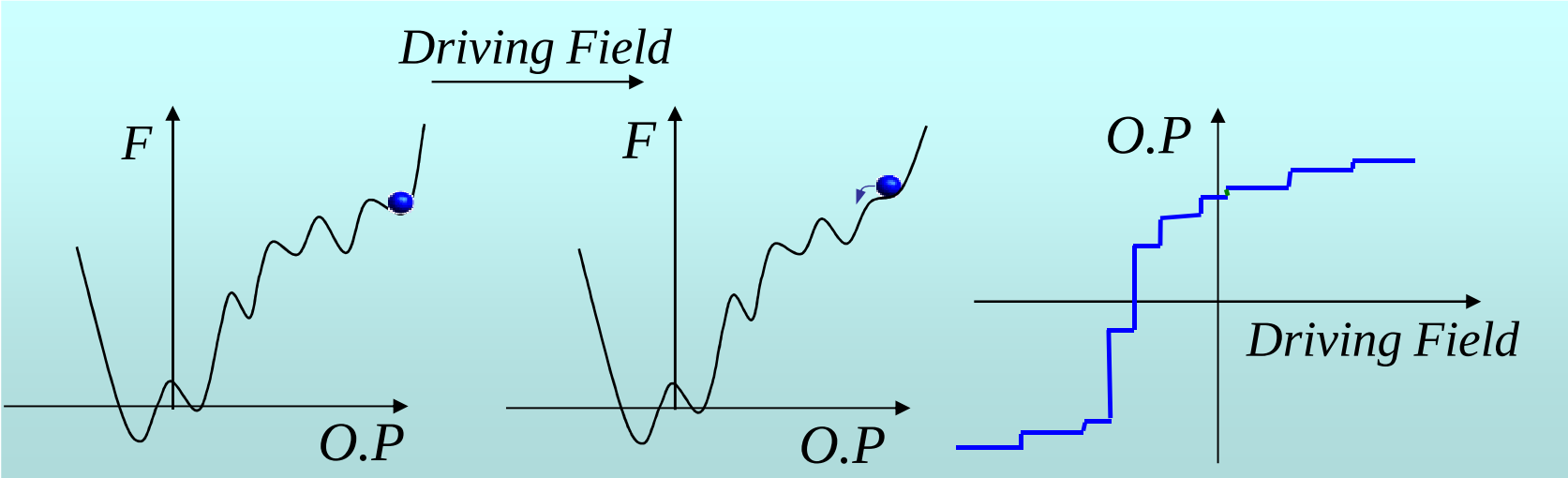

APPLIED PHYSICS LETTERS 97, 021907 (2010)

The noise of the needle: Avalanches of a single progressing needle domain in $LaAlO_3$

Richard J. Harrison[a)] and Ekhard K. H. Salje
Department of Earth Sciences, University of Cambridge, Downing Street, Cambridge CB2 3EQ, United Kingdom

(Received 10 May 2010; accepted 11 June 2010; published online 13 July 2010)

The propagation of a single ferroelastic needle domain under weak elastic stress consists of two parts: a continuous front propagation and jerky avalanches. Optical observation and themodynamic analysis show that the continuous behavior is thermally activated. The avalanches follow power law behavior with an energy exponent $\varepsilon = -1.8 \pm 0.2$ in agreement with self-similar avalanches close to the depinning threshold. Our experiments on ferroelastic $LaAlO_3$ exclude nucleation of secondary domains, so that the observed behavior is related exclusively to the statistical behavior of one single needle domain. © *2010 American Institute of Physics*. [doi:10.1063/1.3460170]

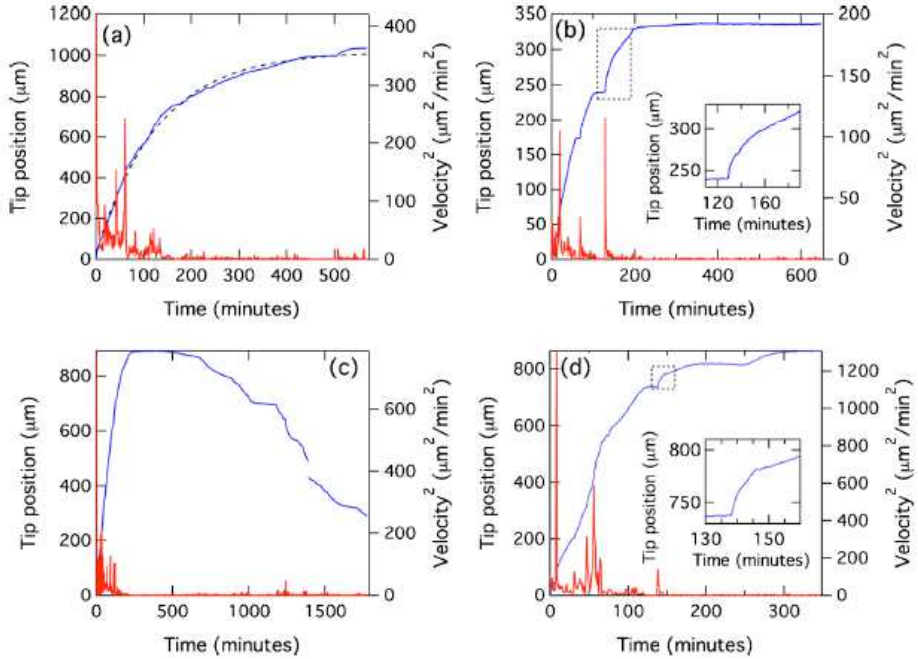

FIG. 1. (Color online) Representative examples of the time evolution of the needle tip position (black line; blue in online version) and the differentiated curve (grey line; red in online version) where the height of each peak measures the energy of the jerk. The insets in (b) and (d) show the depinning transitions near a deep pinning center (expansions of the regions shown by dashed rectangles).

PRL 107, 015702 (2011) PHYSICAL REVIEW LETTERS week ending 1 JULY 2011

Direct Measurement of Microstructural Avalanches during the Martensitic Transition of Cobalt Using Coherent X-Ray Scattering

Christopher Sanborn and Karl F. Ludwig
Department of Physics, Boston University, Boston, Massachusetts 02215, USA

Michael C. Rogers and Mark Sutton
Department of Physics, McGill University, Montreal, Quebec H3A 2T8, Canada
(Received 5 April 2011; published 30 June 2011)

Heterogeneous microscale dynamics in the martensitic phase transition of cobalt is investigated with real-time x-ray scattering. During the transformation of the high-temperature face-centered cubic phase to the low-temperature hexagonal close-packed phase, the structure factor evolution suggests that an initial rapid local transformation is followed by a slower period during which strain relaxes. Coherent x-ray scattering measurements performed during the latter part of the transformation show that the kinetics is dominated by discontinuous sudden changes—avalanches. The spatial size of observed avalanches varies widely, from 100 nm to 10 μm, the size of the x-ray beam. An empirical avalanche amplitude quantifies this behavior, exhibiting a power-law distribution. The avalanche rate decreases with inverse time since the onset of the transformation.

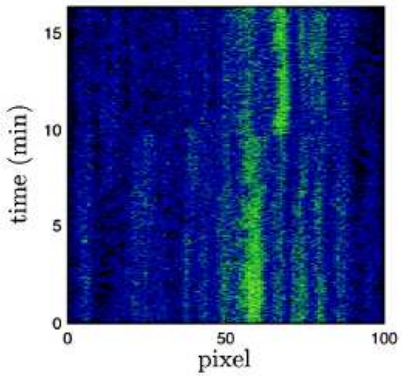

FIG. 2 (color online). A waterfall plot showing the evolution of a 100 pixel cross section of a speckle pattern near the $(00.2)_{hcp}$ peak during a phase transformation. Abrupt changes in pixel intensity such as the one at approximately 10 min indicate the occurrence of avalanches. A smaller avalanche occurs at approximately 7 min.

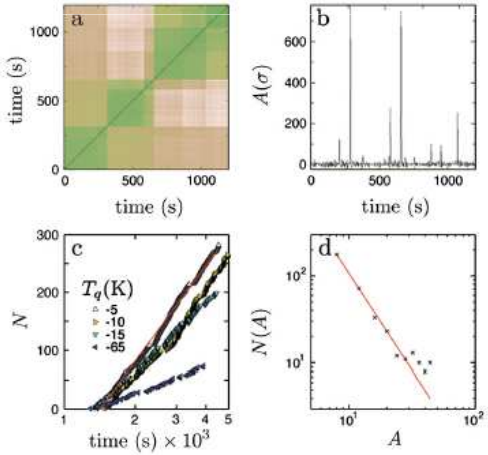

FIG. 3 (color online). (a) The two-time difference values for a quench to $T_q = -5$ K. (b) Avalanche amplitudes calculated from the data in (a). (c) The cumulative number of avalanches over time $N(t)$ near the $(01.3)_{hcp}$ peak for various T_q. The line is a fit of the logarithmic function to the $T_q = -5$ K data. (d) A typical distribution of avalanche amplitudes during a phase transformation with a power-law fit of the data.

PHYSICAL REVIEW B **81**, 174102 (2010)

Avalanche criticality in the martensitic transition of $Cu_{67.64}Zn_{16.71}Al_{15.65}$ shape-memory alloy: A calorimetric and acoustic emission study

María Carmen Gallardo,* Julia Manchado, Francisco Javier Romero, and Jaime del Cerro
Departamento de Física de la Materia Condensada, Universidad de Sevilla, P.O. Box 1065, E-41080 Sevilla, Andalucia, Spain

Ekhard K. H. Salje
Department of Earth Sciences, University of Cambridge, Downing Street, Cambridge CB2 3EQ, United Kingdom

Antoni Planes
Departament d'Estructura i Constituents de la Matèria, Facultat de Física, Universitat de Barcelona, Diagonal 647, E-08028 Barcelona, Catalonia, Spain

Eduard Vives
Department of Physics, University of Warwick, Coventry CV4 7AL, United Kingdom

Ricardo Romero and Marcelo Stipcich
IFIMAT, Universidad del Centro de la Provincia de Buenos Aires, Pinto 399, 7000 Tandil, Argentina
(Received 25 November 2009; revised manuscript received 18 February 2010; published 3 May 2010)

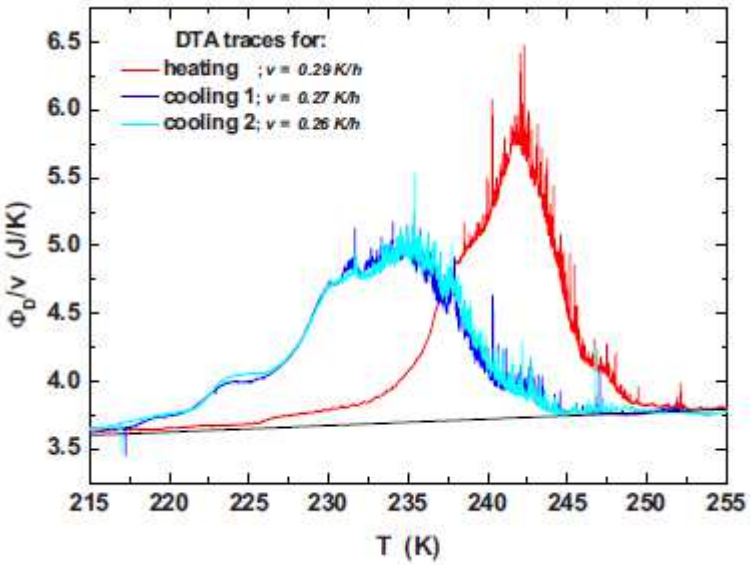

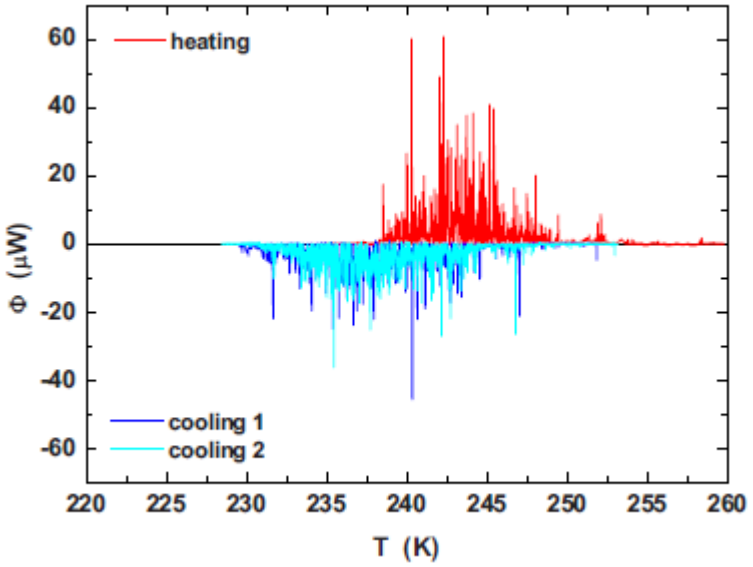

AE signals

Martensitic transition of a Cu-Zn-Al alloy

Sampling rate: 2 MHz

Waiting times ÷ 20

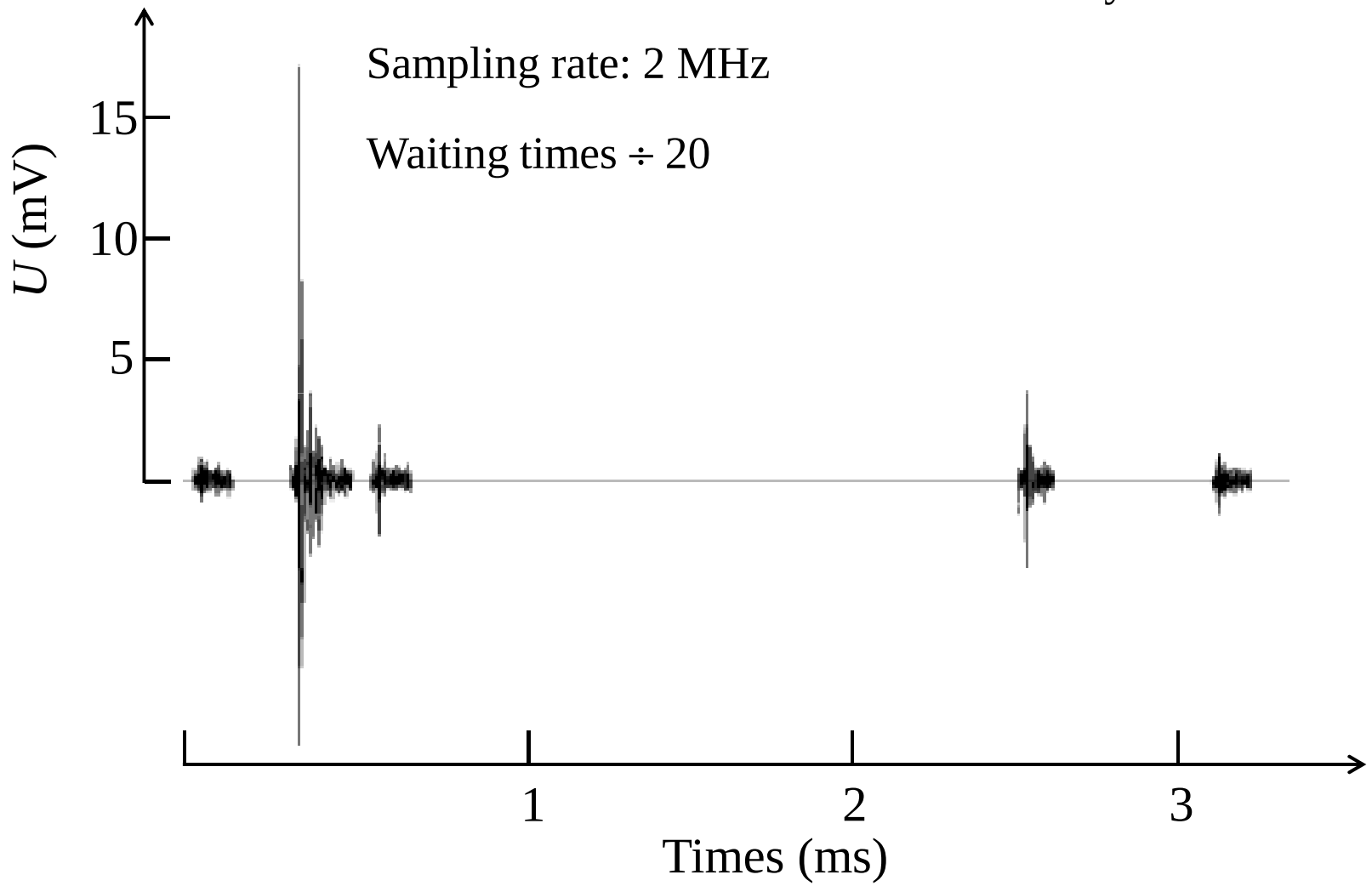

Acoustic and optical activity (2d)

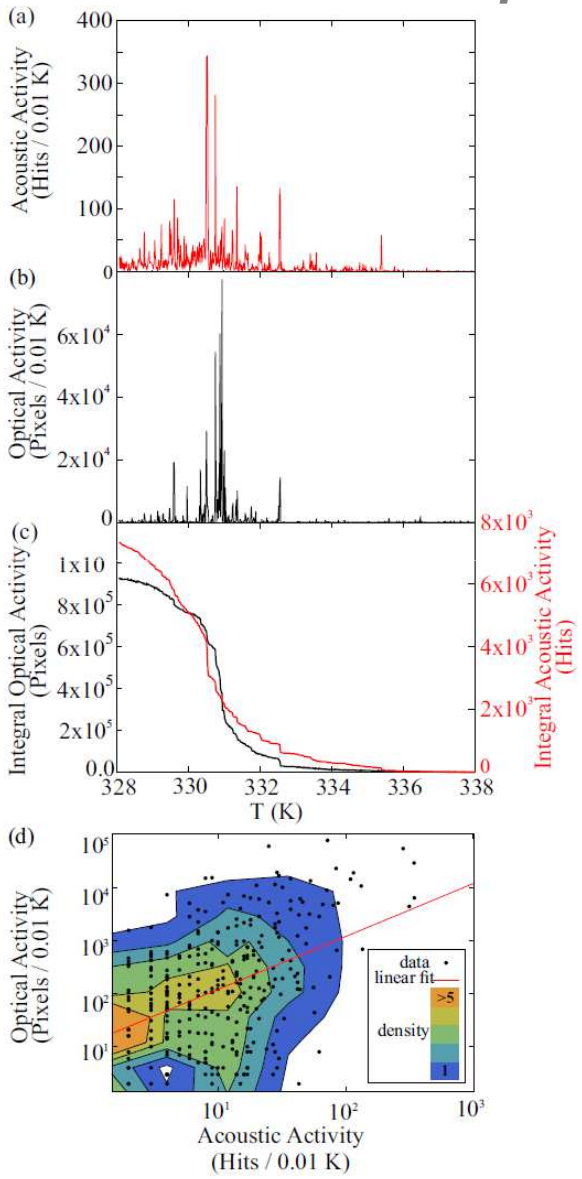

Niemann et al., PRB, **89**, 216118 (2014)

Acoustic and optical activity (2d)

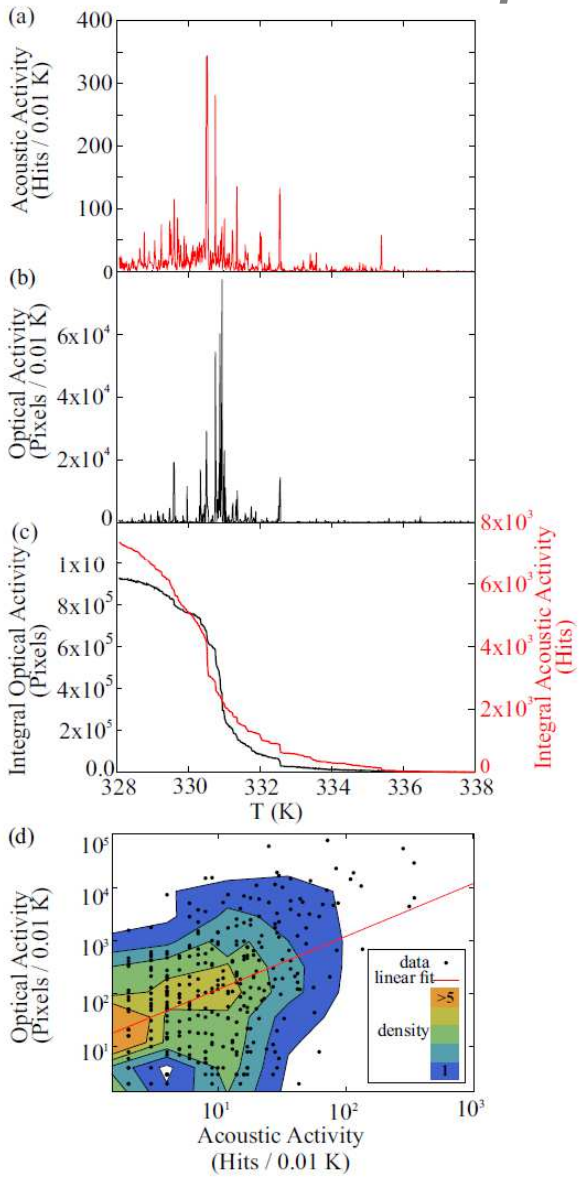

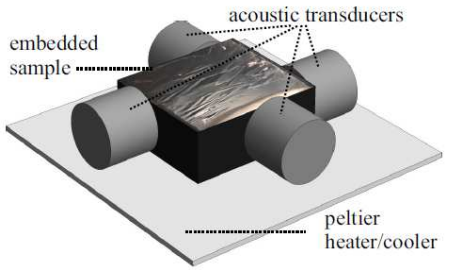

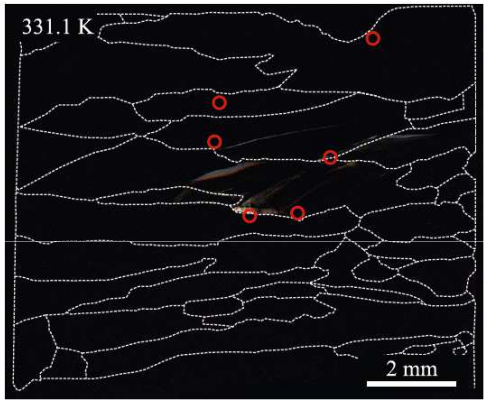

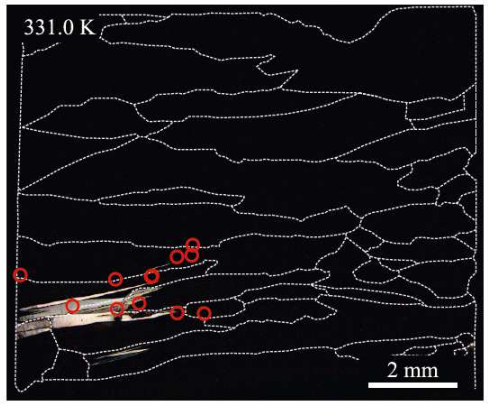

Niemann et al., PRB, **89**, 216118 (2014)

Cycling across the transition

Cu-Al-Mn, single crystal: Cubic → orthorhombic

Annealed at 800 ºC, cooled in air down to RT and cycled

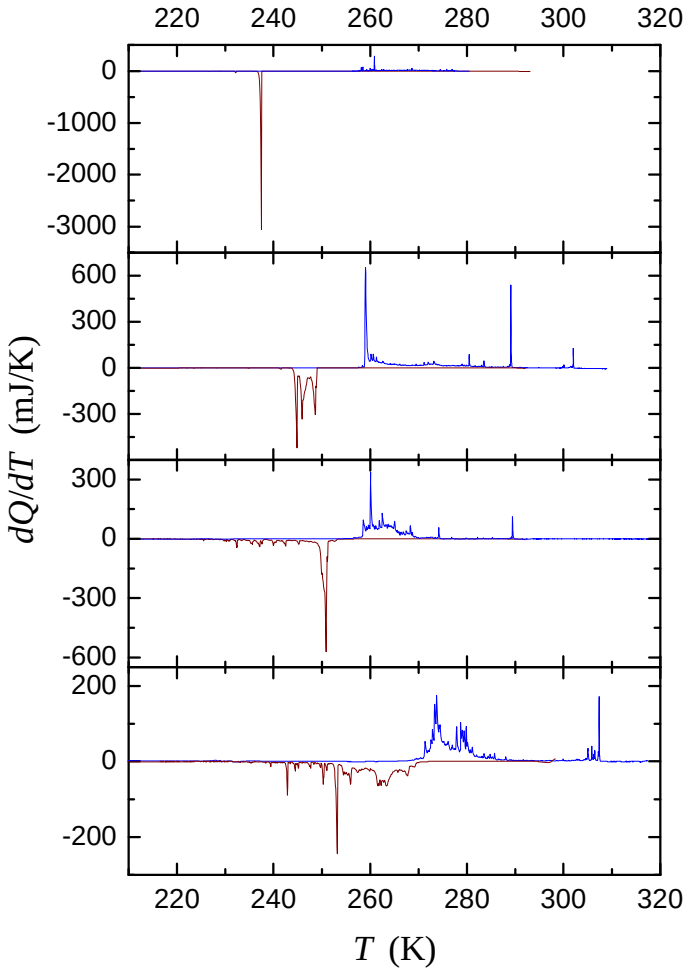

$n = 1$

$n = 2$

$n = 9$

$n = 24$

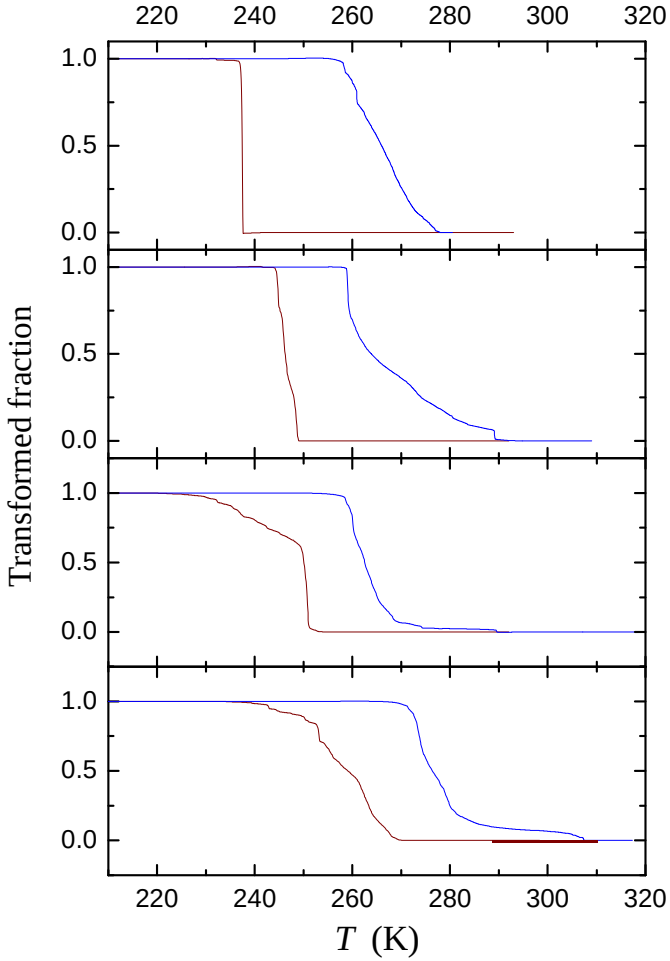

Pérez-Reche et al., PRB, **69**, 064101 (2004)

Cycling: Acoustic emission

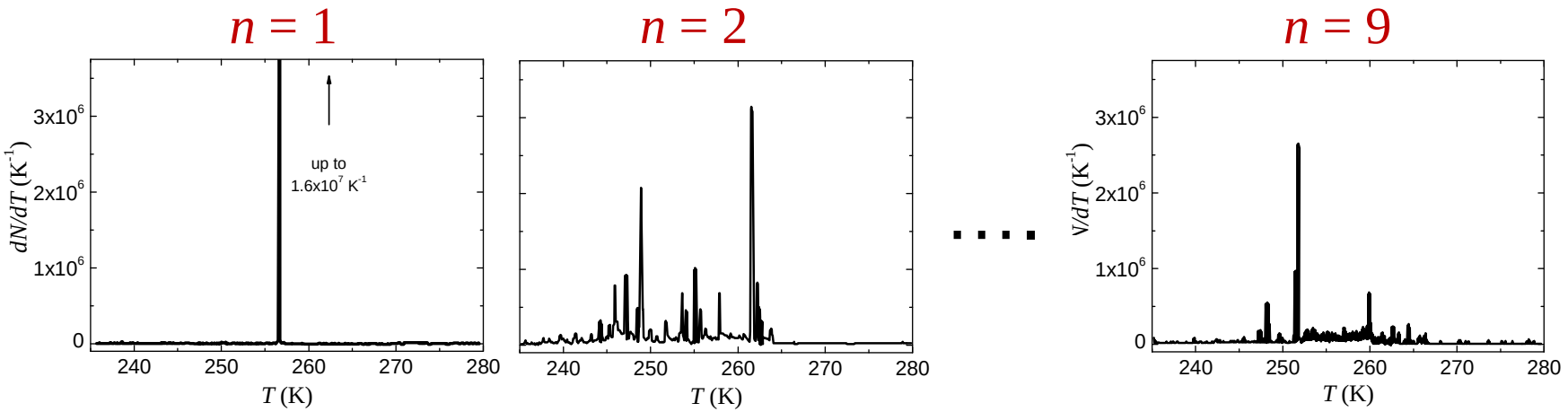

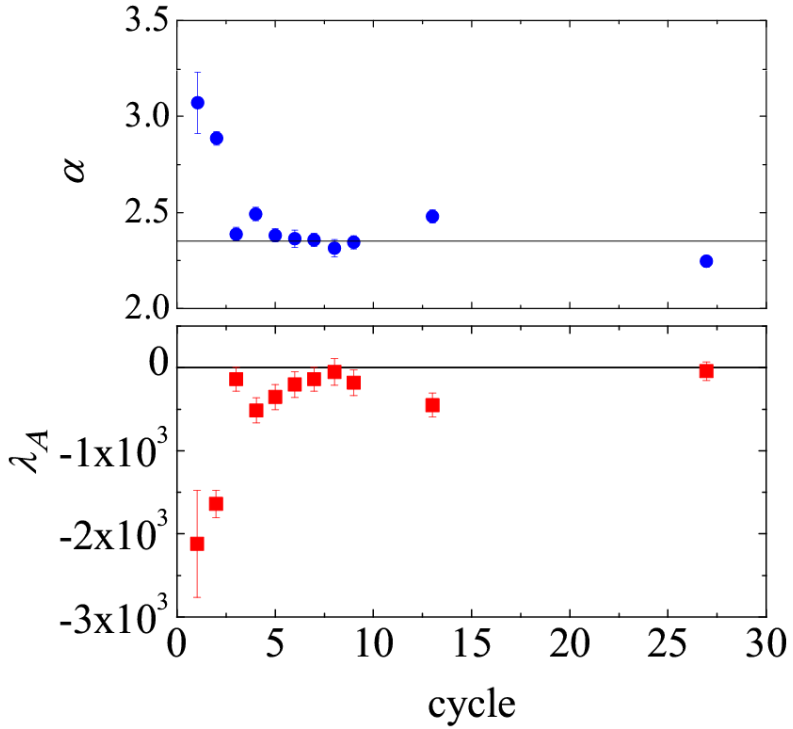

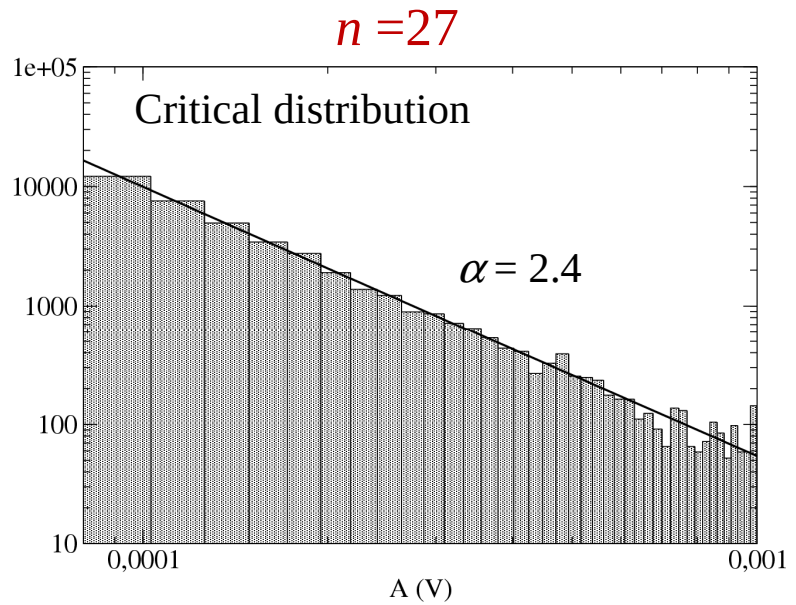

Universality

Cu-based SMA (single & polycrystals)

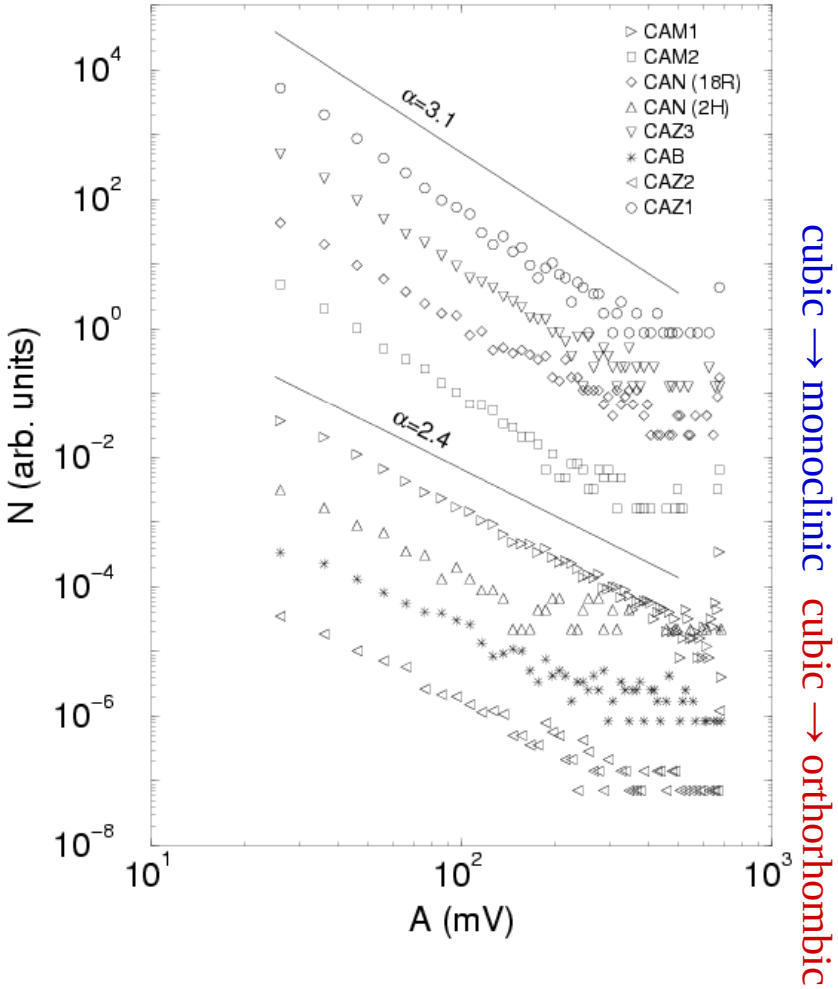

Symmetry	α	ε
Monoclinic	3.0 ± 0.2	2.0 ± 0.2
Orthorhombic	2.4 ± 0.1	-
Tetragonal	2.0 ± 0.3	1.6 ± 0.1

$$z = \frac{\alpha - 1}{\varepsilon - 1} \Rightarrow E \sim A^2$$

Universality

Cu-based SMA (single & polycrystals)

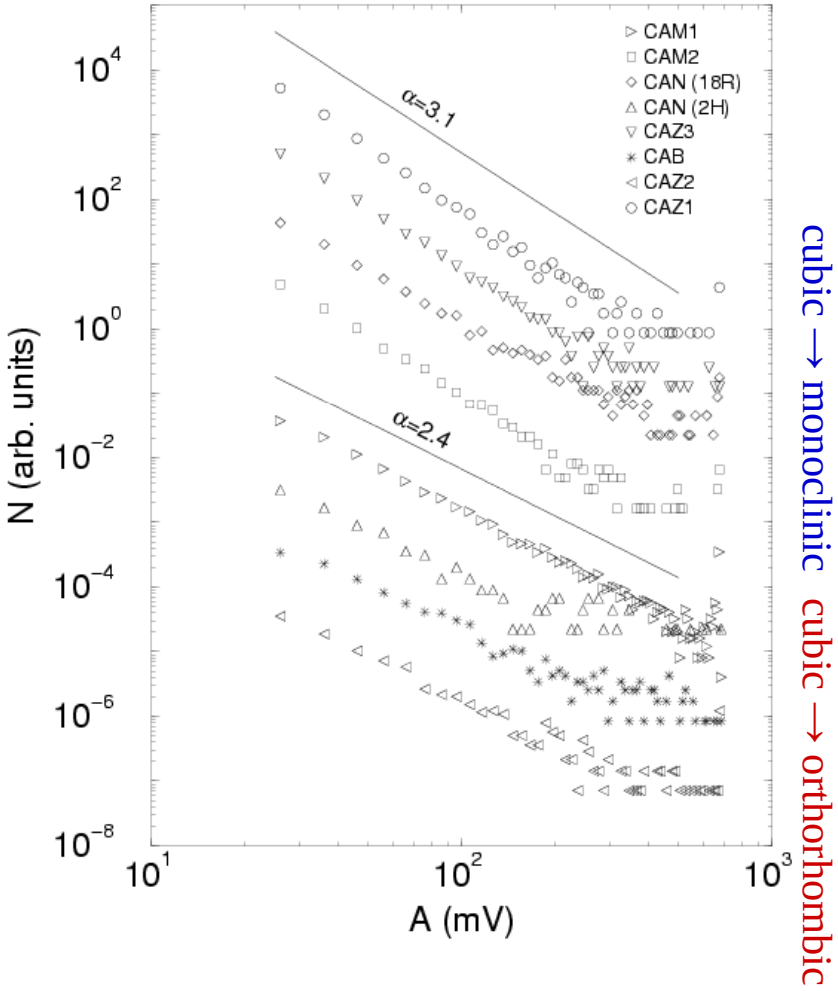

Symmetry	α	ε
Monoclinic	3.0 ± 0.2	2.0 ± 0.2
Orthorhombic	2.4 ± 0.1	1.7 ± 0.2
Tetragonal	2.0 ± 0.3	1.6 ± 0.1

$$z = \frac{\alpha - 1}{\varepsilon - 1} \Rightarrow E \sim A^2$$

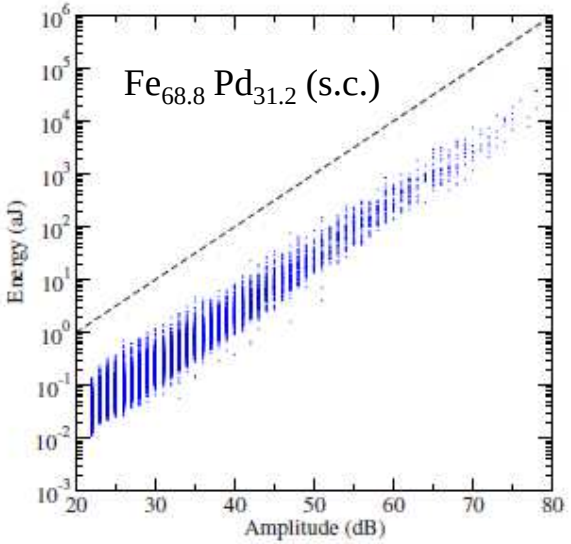

Mixture of phases

Cu-Al-Ni: transformation to a mixture of 18*R* (monoclinic) and 2*H* (orthorhombic) phases.

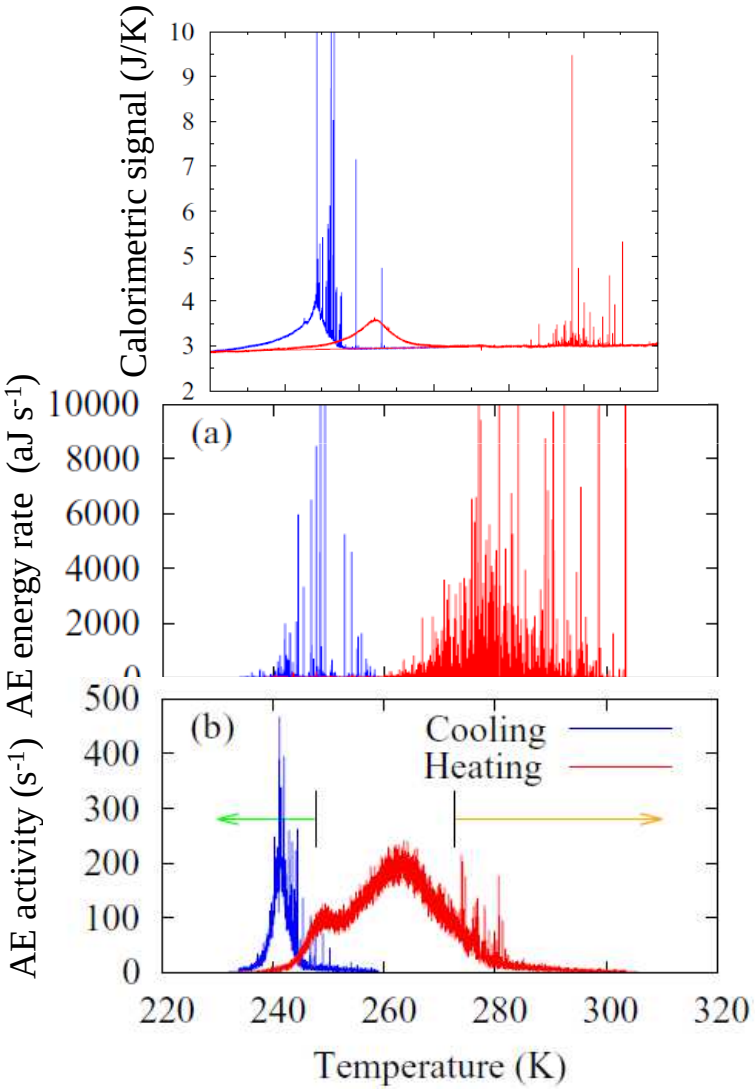

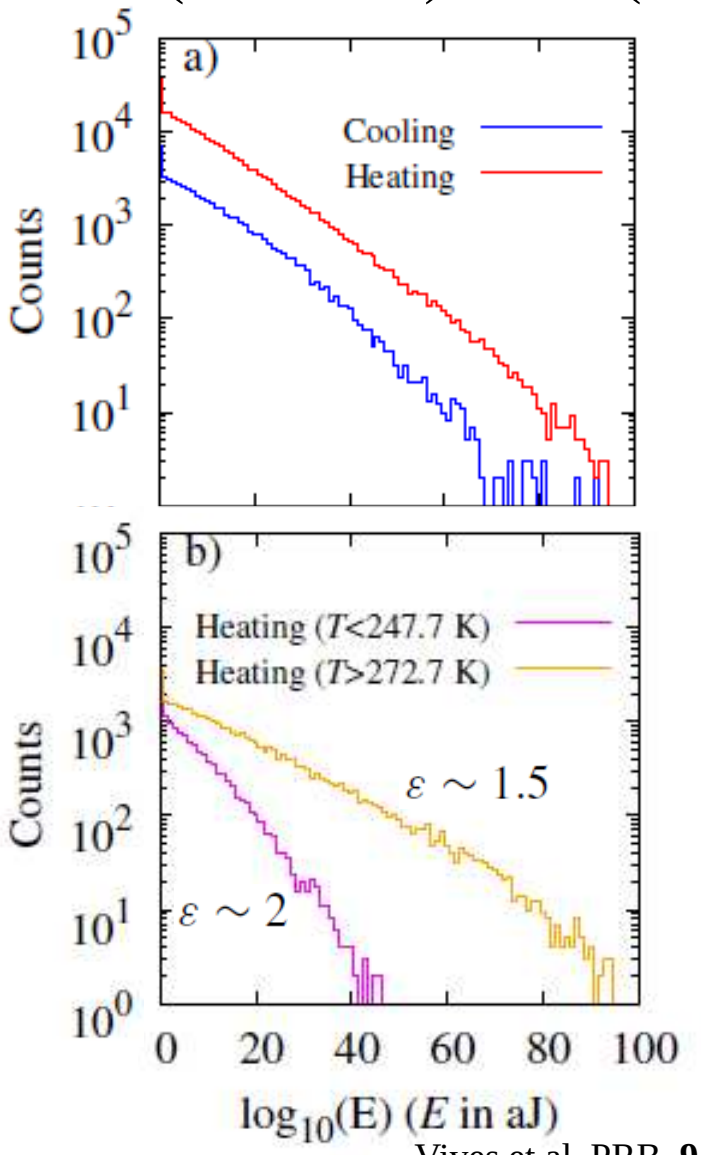

Vives et al, PRB, **94**, 024102 (2016)

Statistics at different scales

Cu-Zn-Al, polycrystal: Cubic → monoclinic

Acoustic Emission vs. Calorimetry

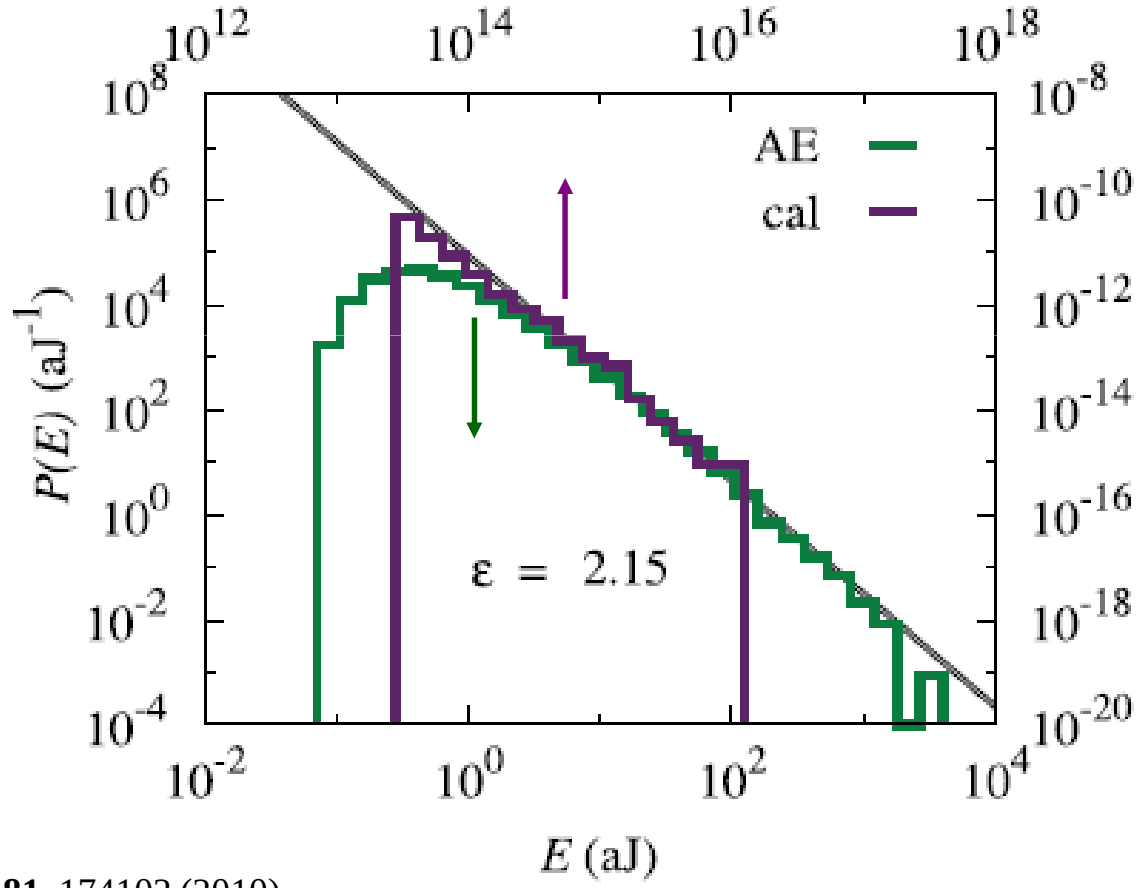

Gallardo et al, PRB, **81**, 174102 (2010)
Baró et al, JPCM, **26**, 126401 (2014)

Stress- vs. strain-induced MT

PRL 101, 230601 (2008) PHYSICAL REVIEW LETTERS week ending 5 DECEMBER 2008

Driving-Induced Crossover: From Classical Criticality to Self-Organized Criticality

Francisco-José Pérez-Reche,[1,2,*] Lev Truskinovsky,[2] and Giovanni Zanzotto[3]

[1]*Department of Chemistry, University of Cambridge, Cambridge, CB2 1EW, United Kingdom*
[2]*Laboratoire de Mécanique des Solides, CNRS UMR-7649, Ecole Polytechnique, Route de Saclay, 91128 Palaiseau, France*
[3]*Dipartimento di Metodi e Modelli Matematici per le Scienze Applicate, Università di Padova, Via Trieste 63, 35121 Padova, Italy*

(Received 10 July 2008; revised manuscript received 4 November 2008; published 2 December 2008)

We propose a spin model with quenched disorder which exhibits in slow driving two drastically different types of critical nonequilibrium steady states. One of them corresponds to classical criticality requiring fine-tuning of the disorder. The other is a self-organized criticality which is insensitive to disorder. The crossover between the two types of criticality is determined by the mode of driving. As one moves from "soft" to "hard" driving the universality class of the critical point changes from a classical order-disorder to a quenched Edwards-Wilkinson universality class. The model is viewed as prototypical for a broad class of physical phenomena ranging from magnetism to earthquakes.

DOI: 10.1103/PhysRevLett.101.230601 PACS numbers: 05.70.Jk, 64.60.av, 64.60.My, 64.70.K−

Stress- vs. strain-induced MT

PRL 101, 230601 (2008) PHYSICAL REVIEW LETTERS week ending 5 DECEMBER 2008

Driving-Induced Crossover: From Classical Criticality to Self-Organized Criticality

Francisco-José Pérez-Reche,[1,2,*] Lev Truskinovsky,[2] and Giovanni Zanzotto[3]

[1]*Department of Chemistry, University of Cambridge, Cambridge, CB2 1EW, United Kingdom*
[2]*Laboratoire de Mécanique des Solides, CNRS UMR-7649, Ecole Polytechnique, Route de Saclay, 91128 Palaiseau, France*
[3]*Dipartimento di Metodi e Modelli Matematici per le Scienze Applicate, Università di Padova, Via Trieste 63, 35121 Padova, Italy*

(Received 10 July 2008; revised manuscript received 4 November 2008; published 2 December 2008)

We propose a spin model with quenched disorder which exhibits in slow driving two drastically different types of critical nonequilibrium steady states. One of them corresponds to classical criticality requiring fine tuning of the disorder. The other is a self-organized criticality which is insensitive to disorder. The crossover between the two types of criticality is determined by the mode of driving. As one moves from "soft" to "hard" driving the universality class of the critical point changes from a classical order-disorder to a quenched Edwards-Wilkinson universality class. The model is viewed as prototypical for a broad class of physical phenomena ranging from magnetism to earthquakes.

DOI: 10.1103/PhysRevLett.101.230601 PACS numbers: 05.70.Jk, 64.60.av, 64.60.My, 64.70.K−

The crossover between the two types of criticality is determined by the mode of driving. As one moves from "soft" to "hard" driving the universality class of the critical point changes from classical order-disorder to a quenched Edwards-Wilkinson universality class.

Stress- and strain-induced experiments

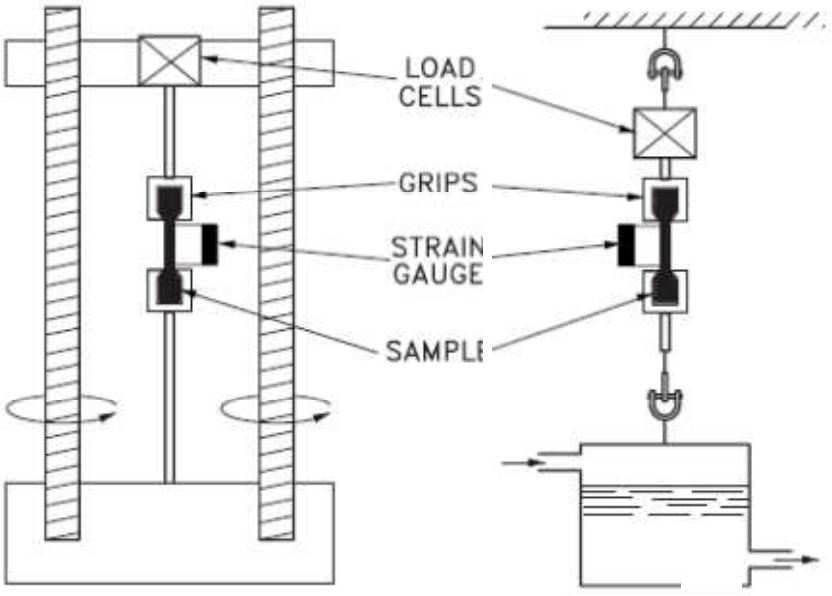

Hard-driving: Strain-controlled experiments

Soft-driving: Stress-controlled experiments

Stress- and strain-induced experiments

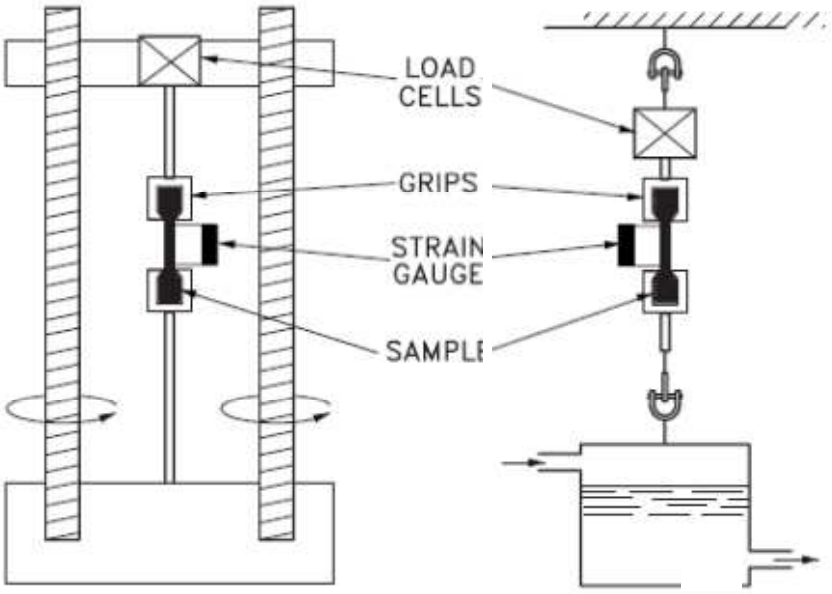

Sample: Cu-Zn-Al, single crystal
Transformation: cubic → monoclinic

Tensile direction: close to the [001] crystallographic direction

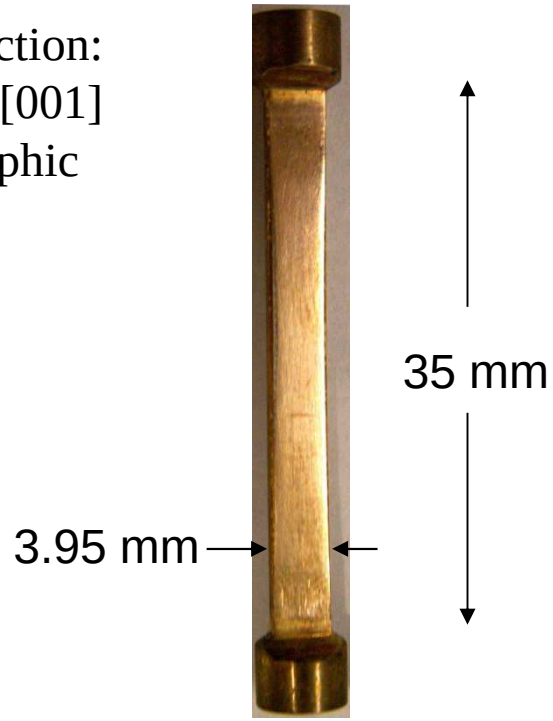

Ø = 5.53 mm²

Hard-driving: Strain-controlled experiments

Soft-driving: Stress-controlled experiments

Stress- and strain-induced experiments

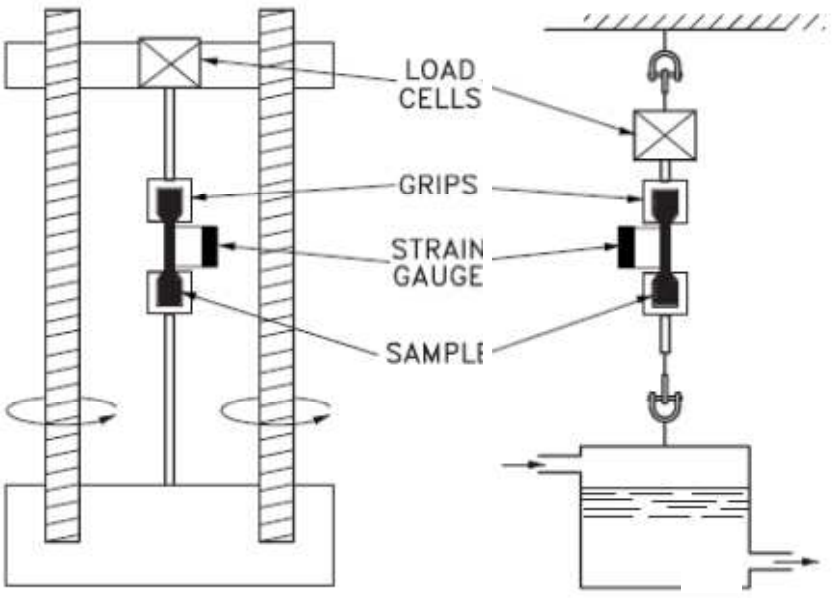

Sample: Cu-Zn-Al, single crystal
Transformation: cubic → monoclinic

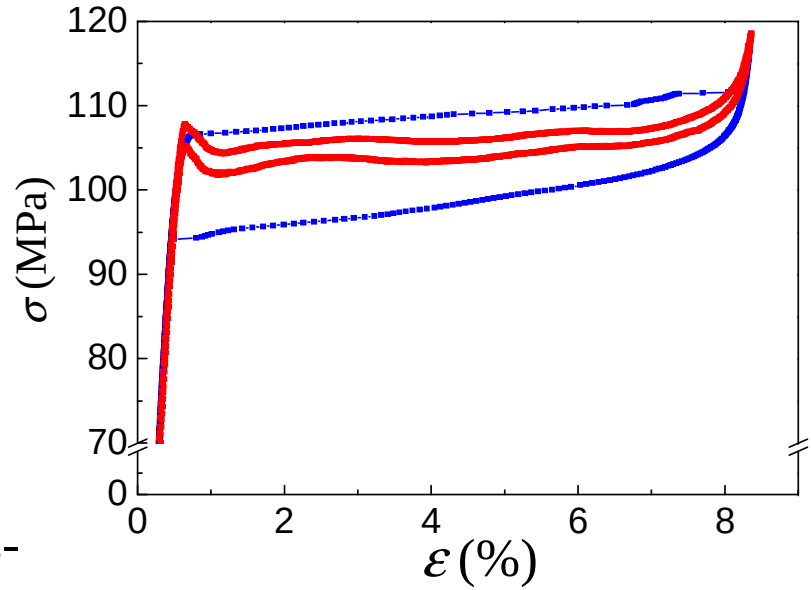

Hard-driving: Strain-controlled experiments

Soft-driving: Stress-controlled experiments

Stress- vs. strain-induced MT

Cu-Zn-Al, single crystal; cubic ($L2_1$) → monoclinic (18M)

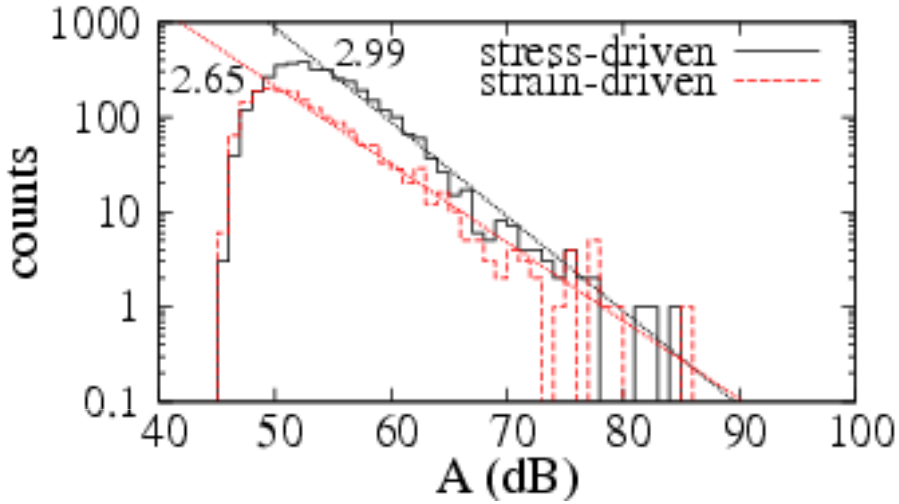

Amplitude distribution

$$N(A)dA \sim A^{-\alpha}\,dA$$

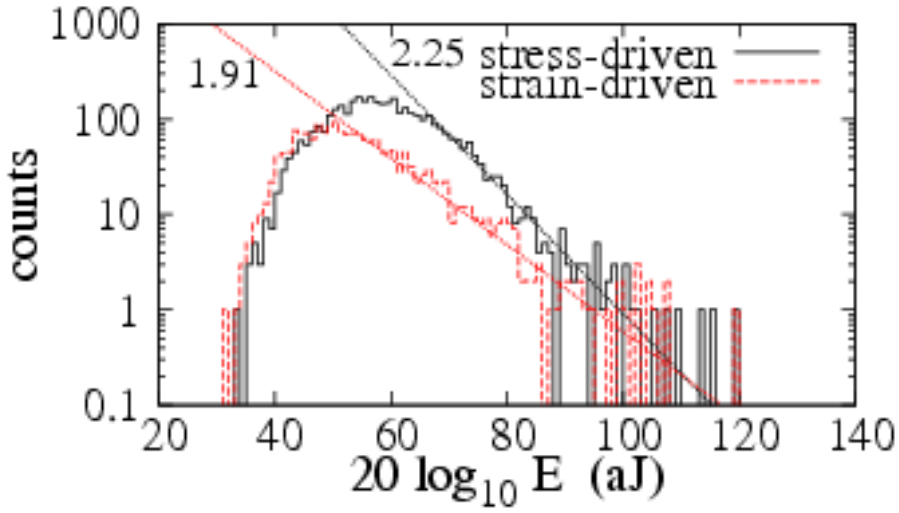

Energy distribution

$$N(E)dE \sim E^{-\varepsilon}\,dE$$

Vives et al., PRB, **80**, 180101(R) (2009)

Evolution with cycling

Cu-Zn-Al, single crystal; cubic ($L2_1$) → monoclinic (18M)

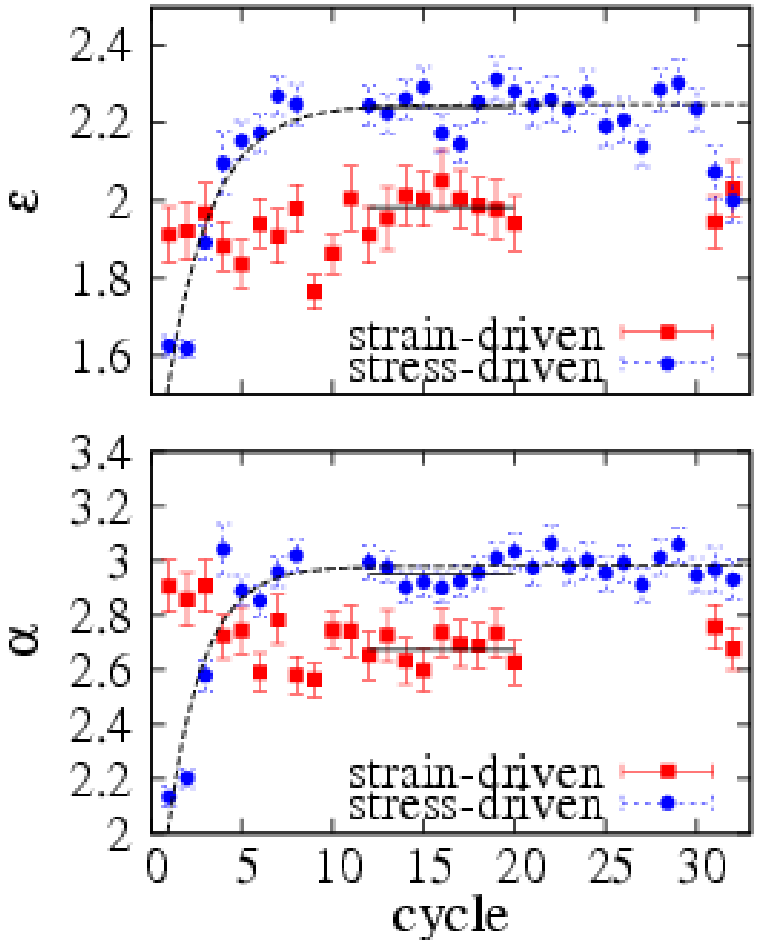

From: Vives et al, PRB **80**, 180101R (2009).

Soft-driving: Evolution during the first cycles ⇒ tuning disorder ⇒ **classical criticality**

Hard-driving: No-evolution ⇒ **self-organized criticalitry**

Driving	ε	α
Hard	1.98 ± 0.03	2.67 ± 0.03
Soft	2.24 ± 0.02	2.95 ± 0.02

Reducing variant multiplicity: magnetic field

$Ni_{52}Mn_{23}Ga_{25}$, single crystal ; cubic ($L2_1$) → monoclinic (10M)

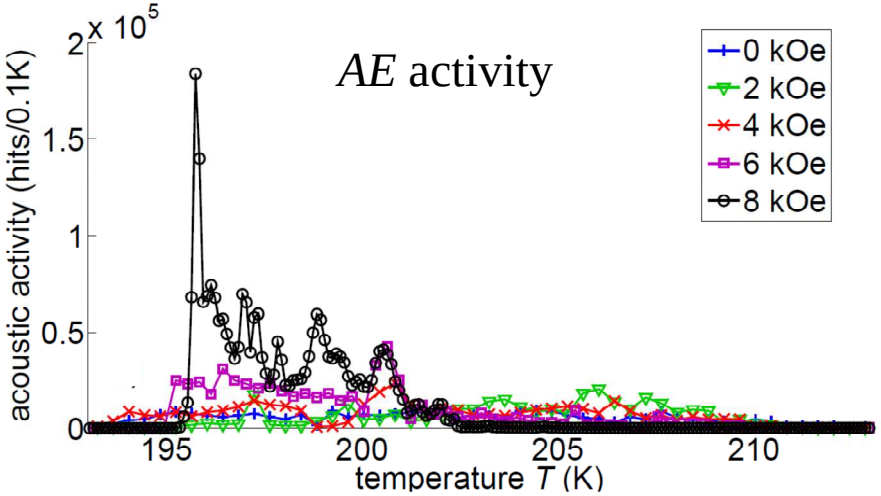

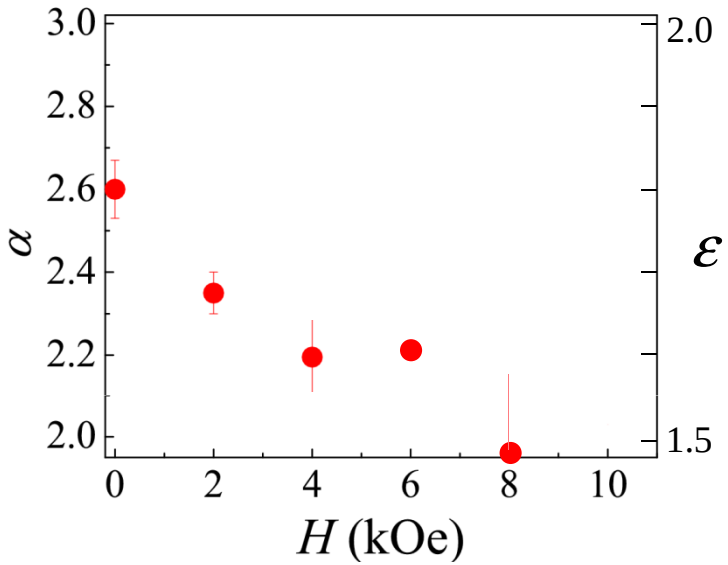

Amplitude distributions

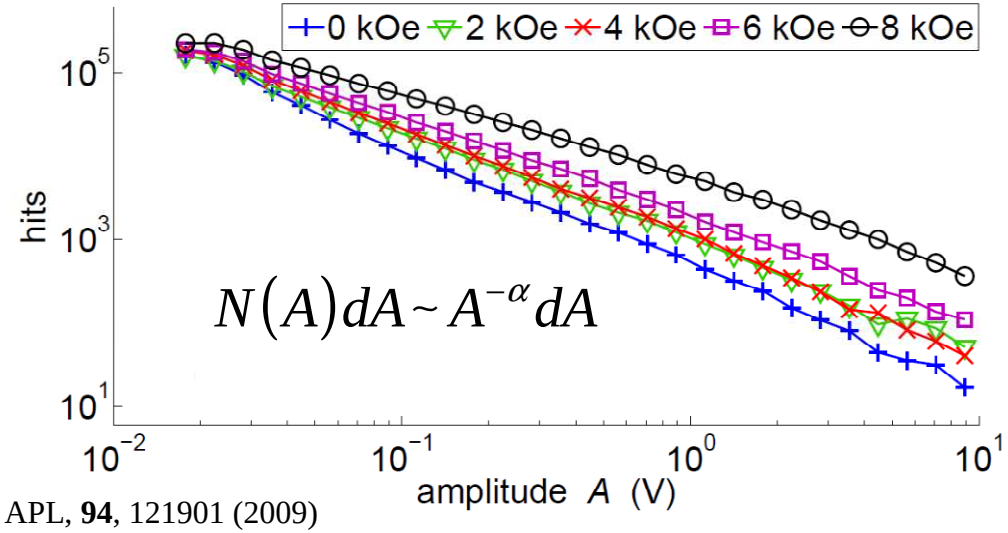

APL, **94**, 121901 (2009)

Reducing variant multiplicity: stress

$Ni_{50.4}Mn_{27.9}Ga_{21.7}$, single crystal ; cubic ($L2_1$) → monoclinic (10M)

AE activity

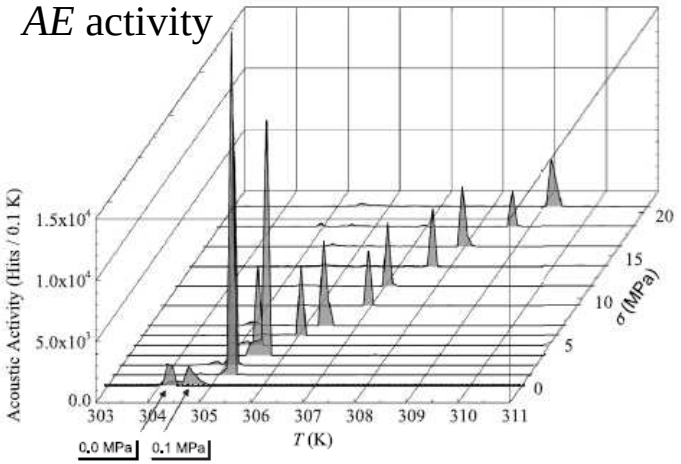

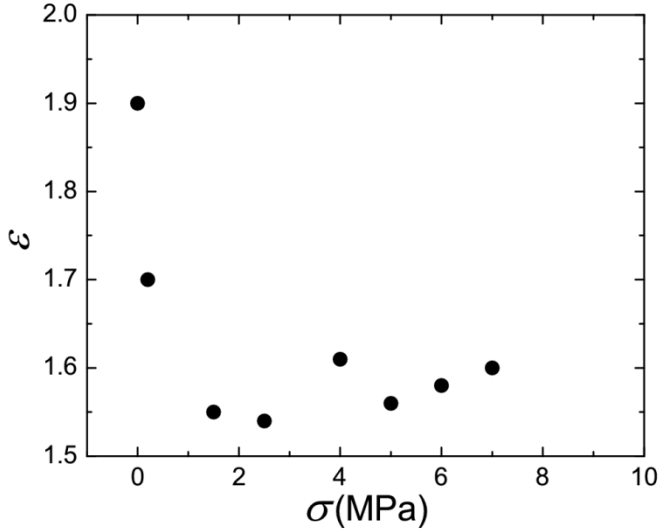

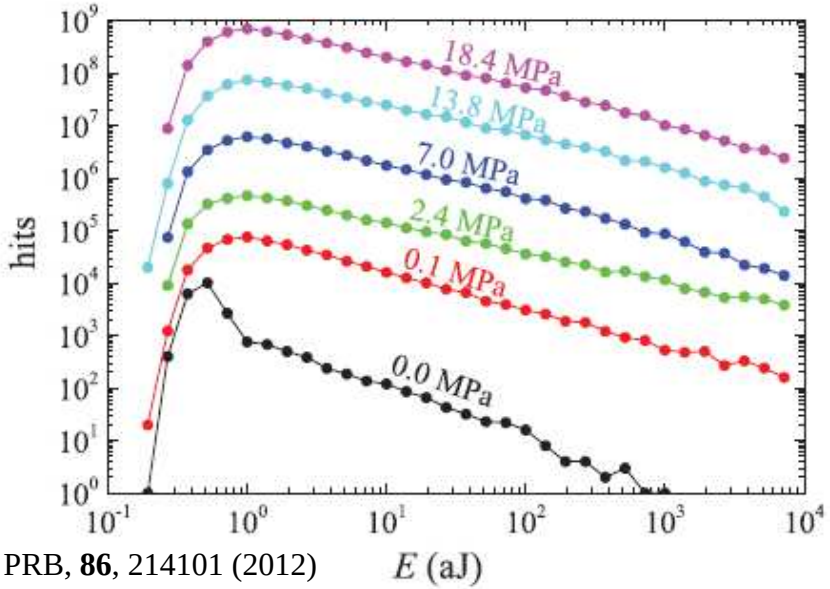

PRB, **86**, 214101 (2012)

Reducing variant multiplicity: stress

$Ni_{50.4}Mn_{27.9}Ga_{21.7}$, single crystal ; cubic ($L2_1$) → monoclinic (10M)

AE activity

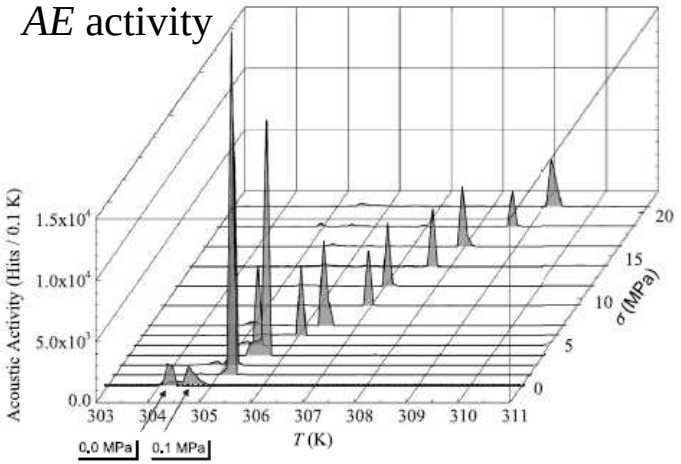

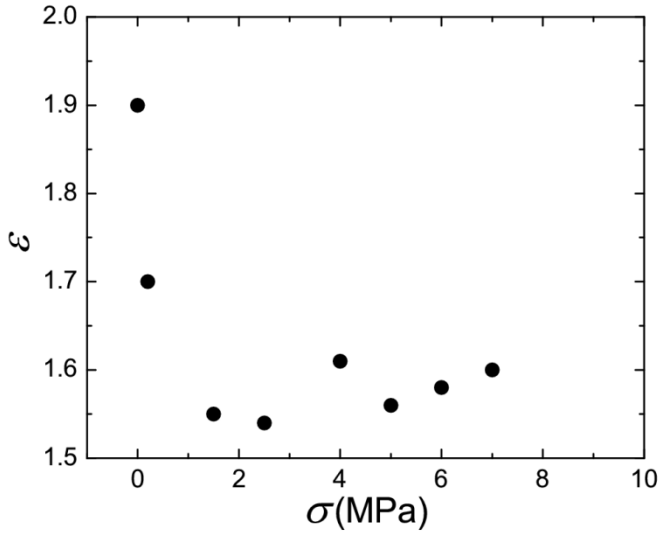

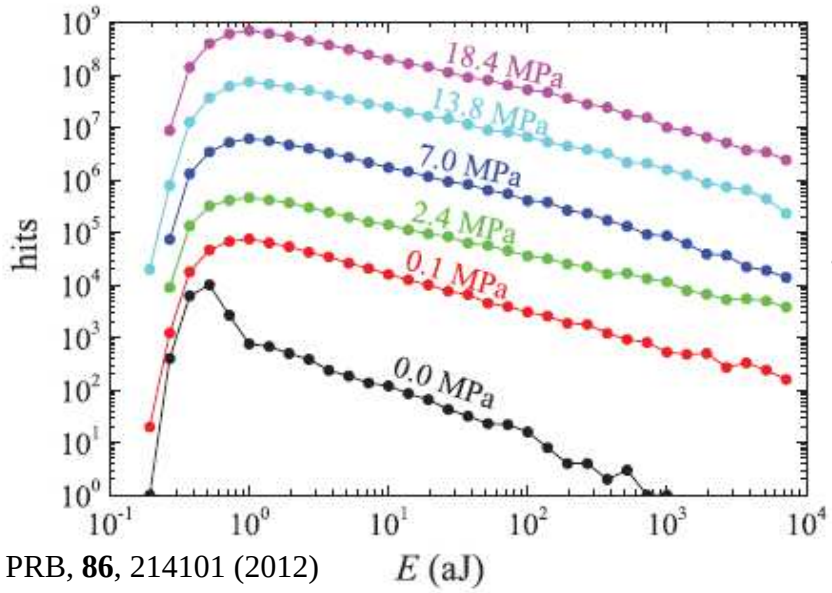

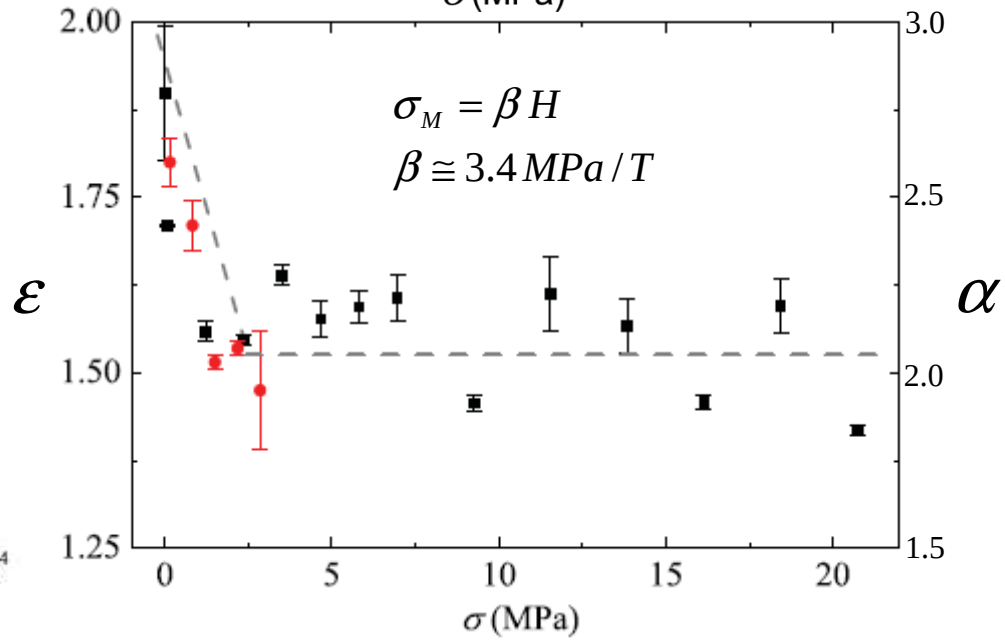

PRB, **86**, 214101 (2012)

Waiting times distribution

Waiting times between events above given energy thresholds are considered

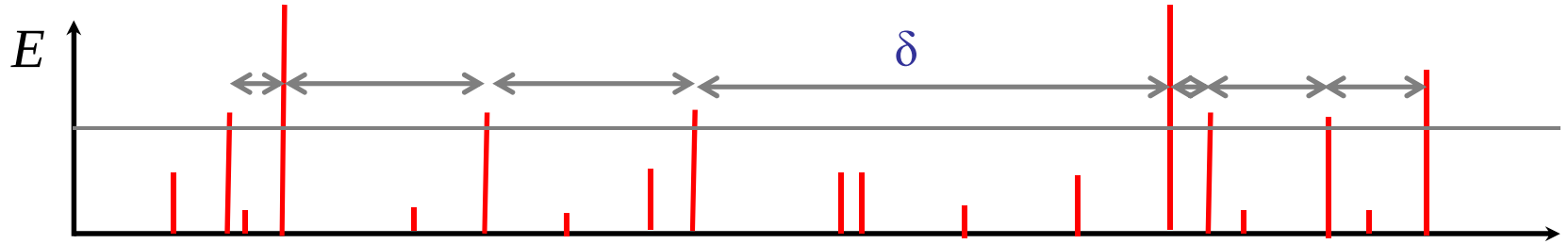

Waiting times (δ) distribution above a minimum of energy (threshold) in different regions is governed only by the mean event activity $\langle r \rangle$ in such a way that the waiting times probability distribution fulfills the following scaling law [P. Bak, et al., *PRL* **88**, 178501 (2002)] :

$$D(\delta) = \langle r \rangle \Phi(\langle r \rangle \delta)$$

The scaling function Φ is expected to show double power-law behaviour:

$$\Phi(x) \propto \begin{cases} x^{-(1-\nu)} & \text{for small arguments } (1\text{-}\nu \sim 1) \text{ (related to correlations)} \\ x^{-(2+\xi)} & \text{for large arguments } (2+\xi > 2) \text{ (related to the distribution of background activity rates)} \end{cases}$$

Waiting times distribution: scaling

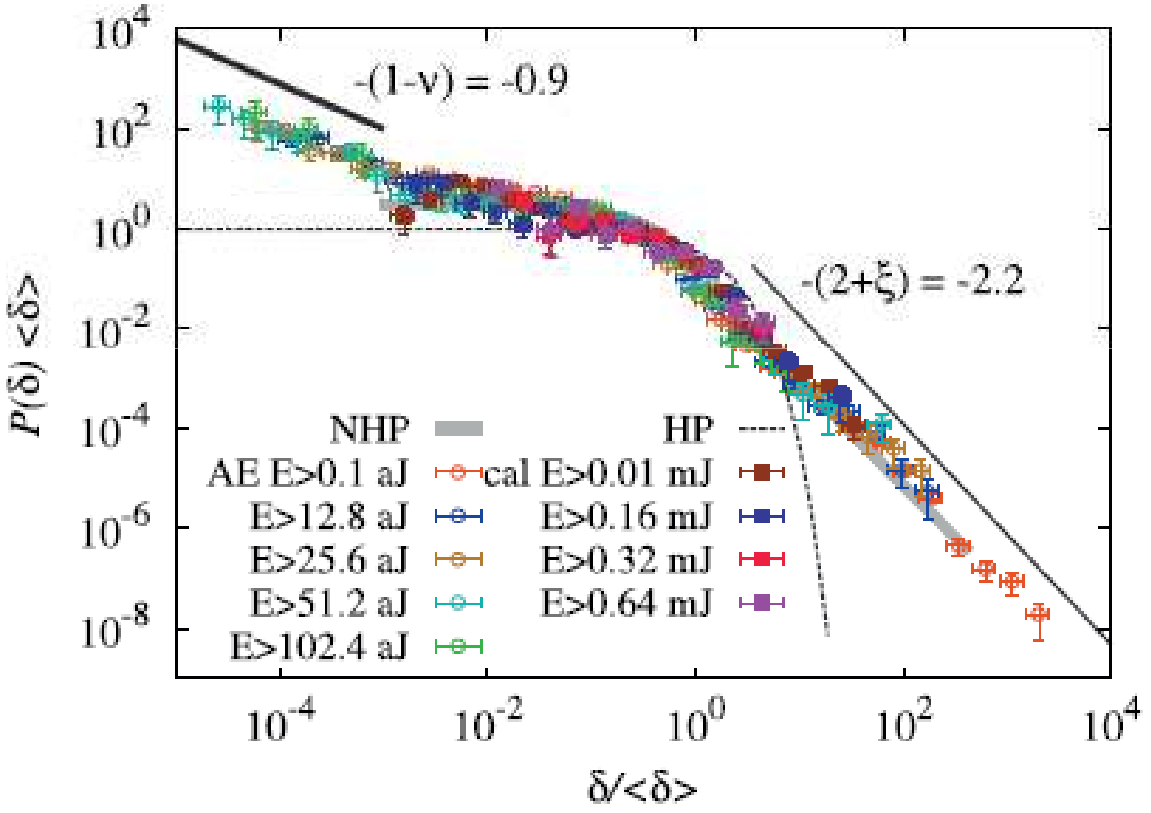

From: Baró et al, JPCM, **26**, 126401 (2014)].

Porous materials under stress

Failure of porous materials under compression stress is usually preceded by significant precursor activity.

Materials:

Non-granular: skeleton containing a network of interconnected nanometer-sized pores with narrow size distribution.

Examples: Vycor, bones, …., porous Ti-Ni

Granular: grains touching (and penetrating) each other. The voids between the grains constitute a random network of interconnected corridors and pockets (wider pore size distribution).

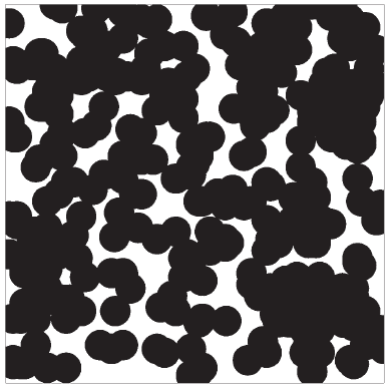

Examples: Gelsil, alumina, berlinite, minerals (goethite, sandstones, …), …

Vycor

Porosity: 40%
Skeleton (> 98% SiO_2)

Mean pore diameter 7.5 nm
Narrow pore size distribution

Typical sample size 5x3x3mm

Experiments

Compression rates *R:* 0.2 kPa/s
1.6 kPa/s
6.5 kPa/s
12.2 kPa/s

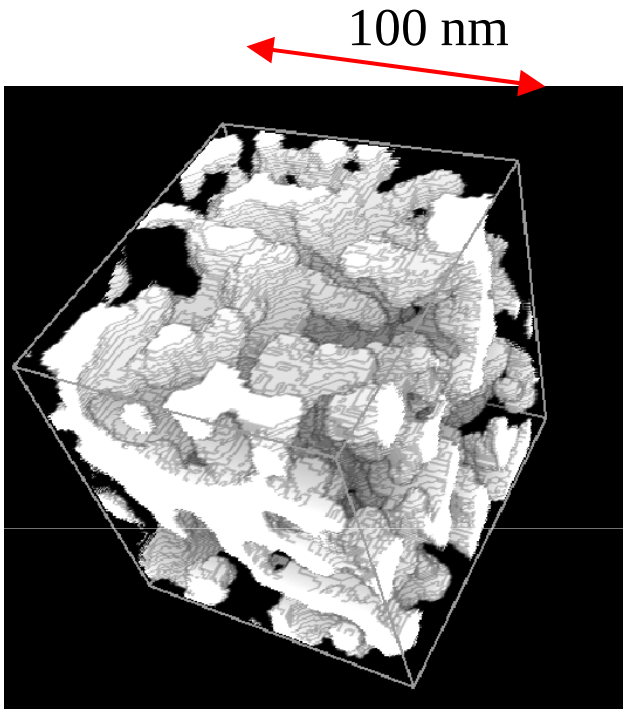

Bentz et al (1998)

Experimental setup

Compression plates with embedded AE piezoelectric transducers

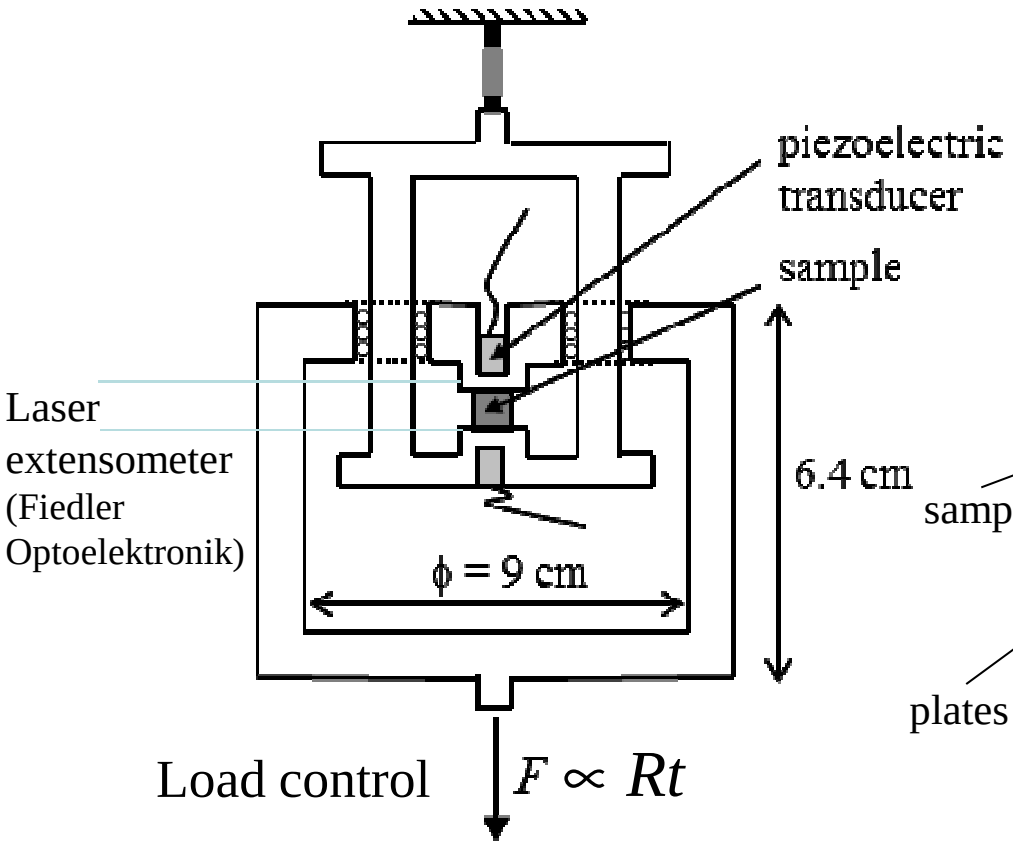

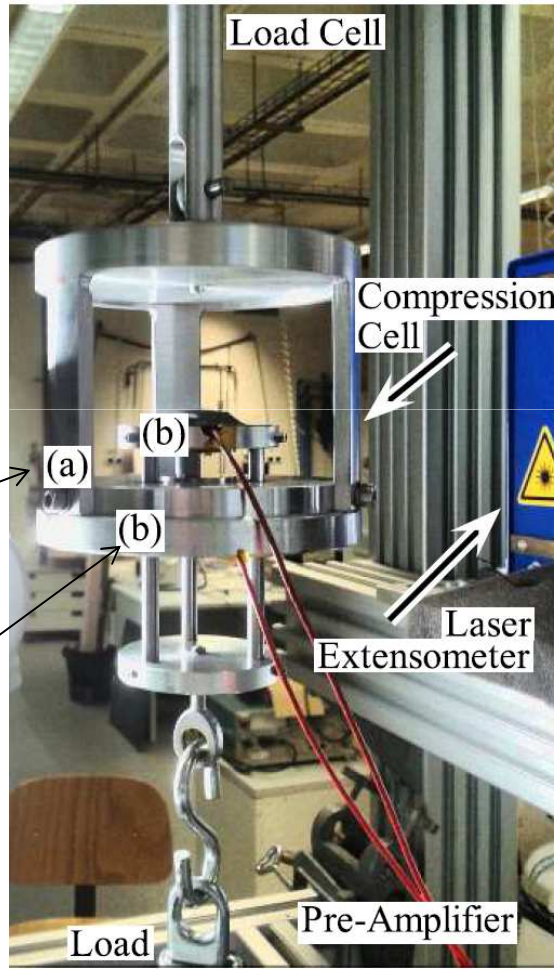

Refs.: Salje et al., Phil. Mag. Lett. **91**, 554–560, (2011)
Salje et al., Am. Min. **98**, 609 (2013)

Example of experiment

Experiment performed in Vycor (40% porosity) at a rate R = 1.6 kPa/s

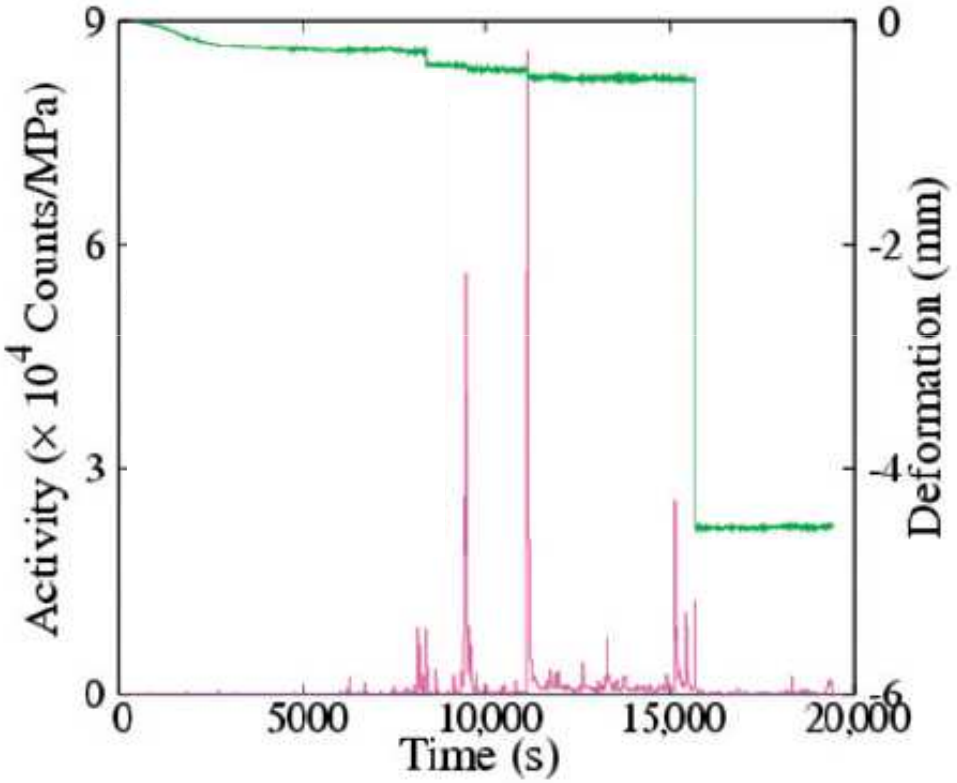

Good correlation between sample height change and AE activity.

Example of experiment

Experiment performed in Vycor (40% porosity) at a rate R = 1.6 kPa/s

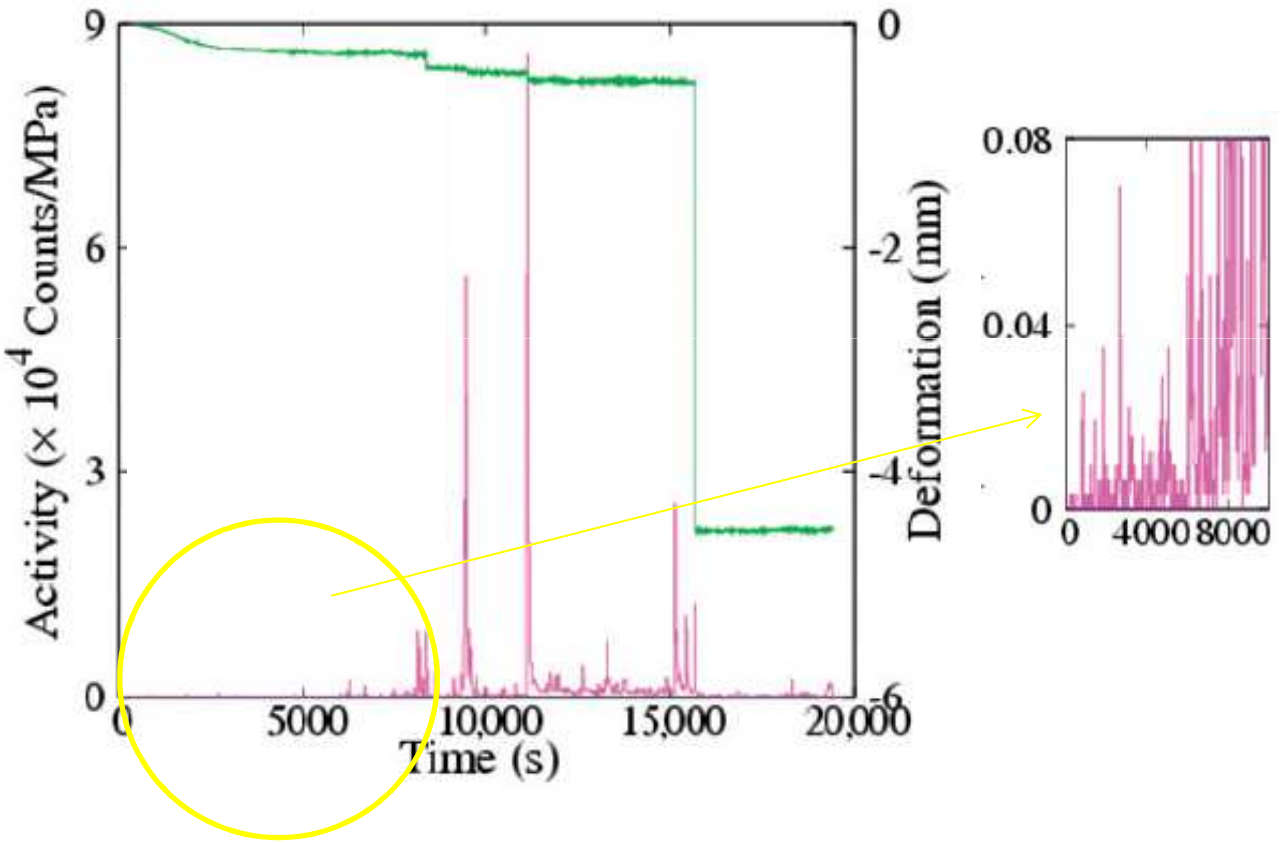

Good correlation between sample height change and AE activity.

AE and earthquakes

Both phenomena occur in very different ranges:

Earthquakes		AE events: *labquakes*
E: 10^{10}-10^{18} J	$\times 10^{-30}$	E: 10^{-18}-10^{-11} J
x:10^{2}- 10^{7} m	$\times 10^{-10}$	x: ? -10^{-3} m
t: 10^{-2}- 10^{6} h	$\times 10^{-7}$	t: 10^{-10} - 10^{0} h
Available catalogues (California, Japan,..)		AE events in compressed Vycor

Statistical analysis:

- **Gutenberg-Richter law: energy distribution**
- Omori law: temporal distribution of aftershocks
- Productivity law: energy dependence of the distribution of aftershocks
- **Unified scaling law for the distribution of waiting times**

These laws are power-laws, indicating the absence of characteristic scales and introducing a set of exponents (ε, p, α, 1-ν and $2+\xi$).

Energy distribution: Gutenberg-Richter law

The log of the number of earthquakes with seismic moment larger than M linearly increases with M : $\log_{10} N_{>M} = a - bM \quad (b \approx 1 \pm 0.1)$

Seismic moment-energy relationship: $\log_{10} E = 3M/2 + 4.8 \Rightarrow$

$$p(E)dE \propto E^{-\varepsilon} dE, \quad \varepsilon = 1 + \frac{2}{3} b \approx 1.67 \pm 0.15$$

Distribution of energies for different time subperiods:

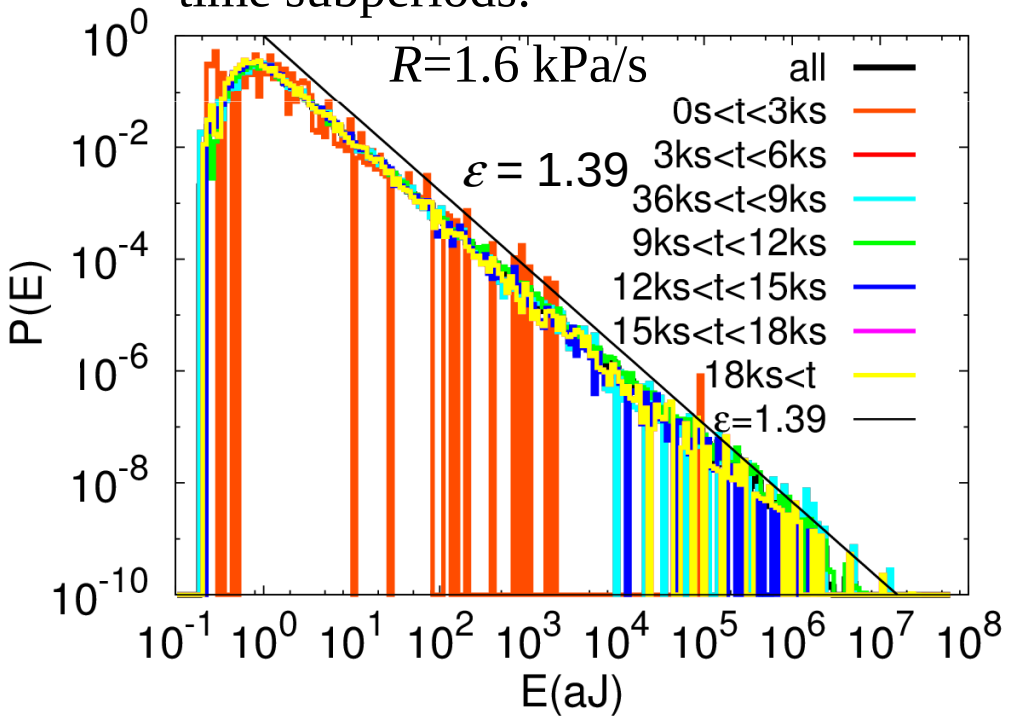

From: Baró et al., *PRL*, **110**, 088702 (2013)

Exponent as function of the minimum cut-off.

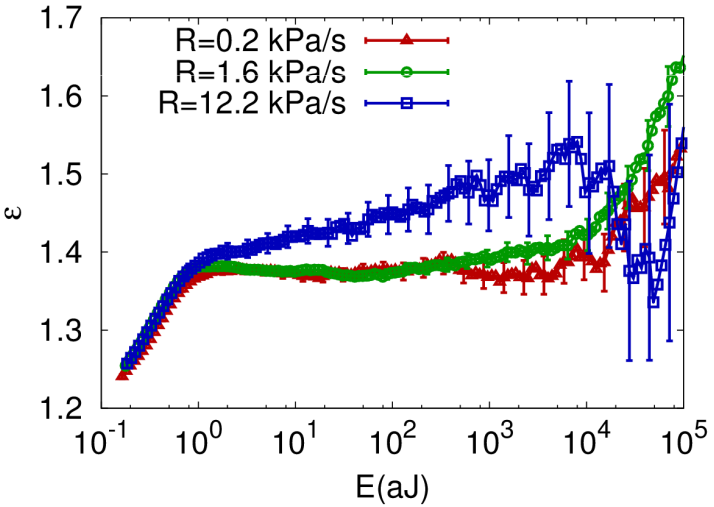

The exponent is fitted using the maximum likelihood method (see: Clauset et al., Siam, **51** (2009)].

Results: Unified scaling law

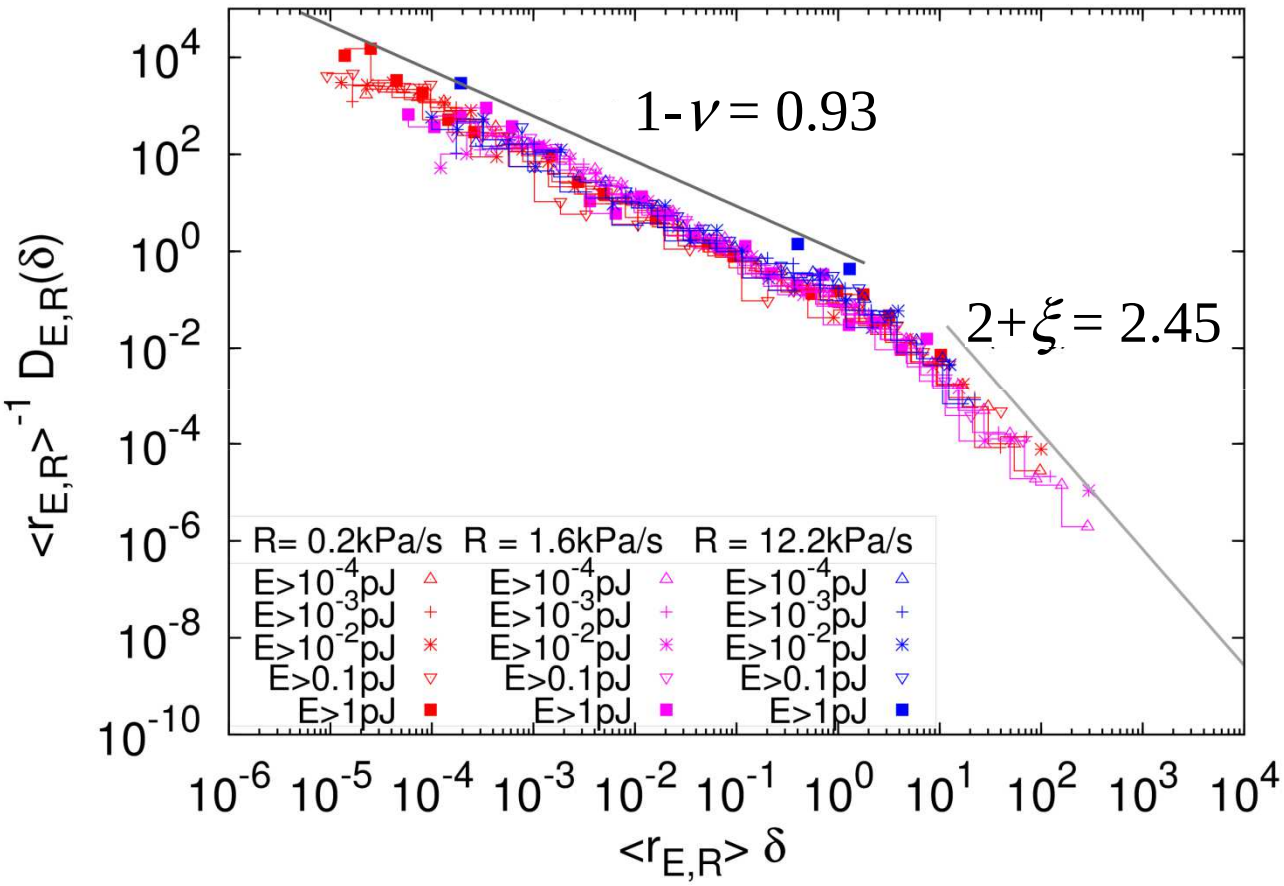

From: Baró et al., *PRL*, **110**, 088702 (2013)

Comparison with eartquakes

Same results including data for earthquakes in California (for different spatial windows) in the period 1981-2011.

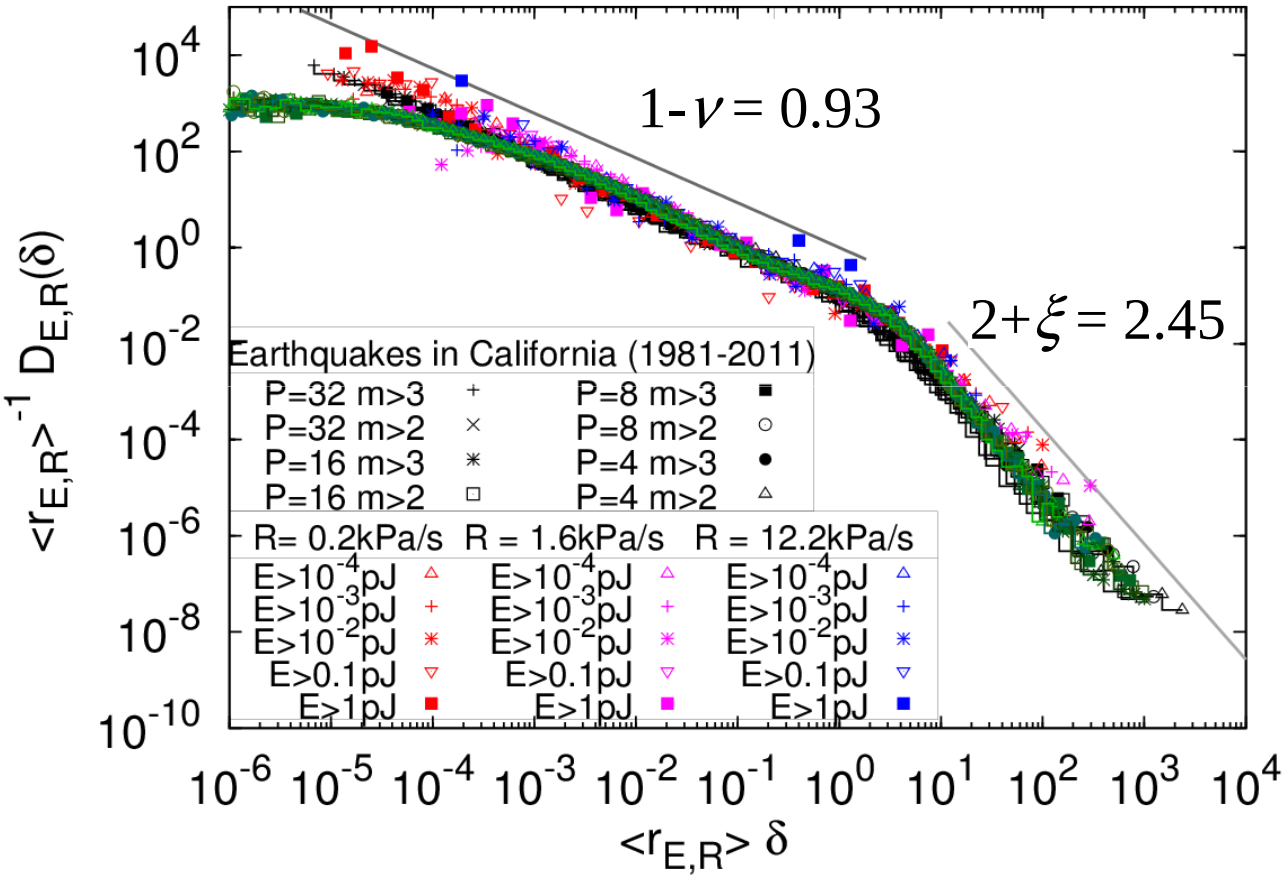

The overlap show that waiting times display same statistics in spite of the disparity of scales.

Summary : earthquakes vs. labquakes

		EARTHQUAKES	LABQUAKES
Gutenber-Richter	ε	1.67±0.15	1.40±0.05
Omori	p	0.9-1.8	0.75
Productivity	α	0.7-0.9	0.5±0.1
Universal scaling function	$1-\nu$	0.9	0.93
	$2+\xi$	2.2	2.45

Excellent fulfillement of fundamental statistical laws of earthquakes by AE events during compression of porous Vycor with **very similar exponents.**

Ref: J. Baró, E. Vives and A. Planes, in *Avalanches in Functional Materials and Geophysics*, ed. By E. K. H. Salje, A. Saxena and A. Planes, Chap. 3, From Labquakes in Porous Materials to Earthquakes, Springer-Verlag, 2017 .

Compression of porous Ti-Ni

SEM image:$Ti_{53.7}Ni_{46.4}$
porosity: 38.9%

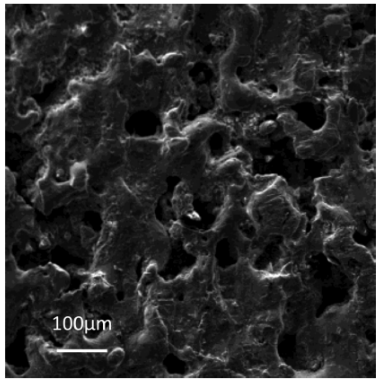

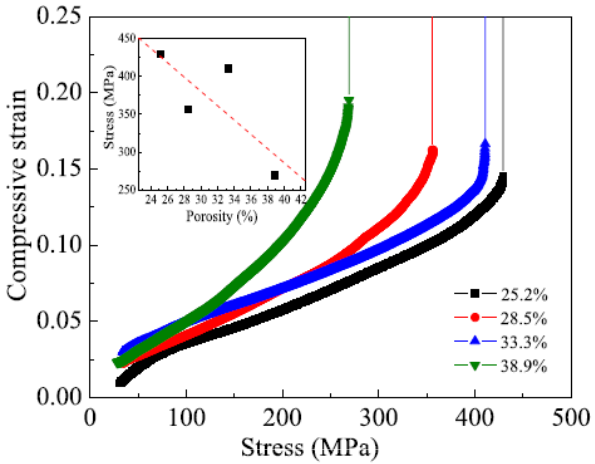

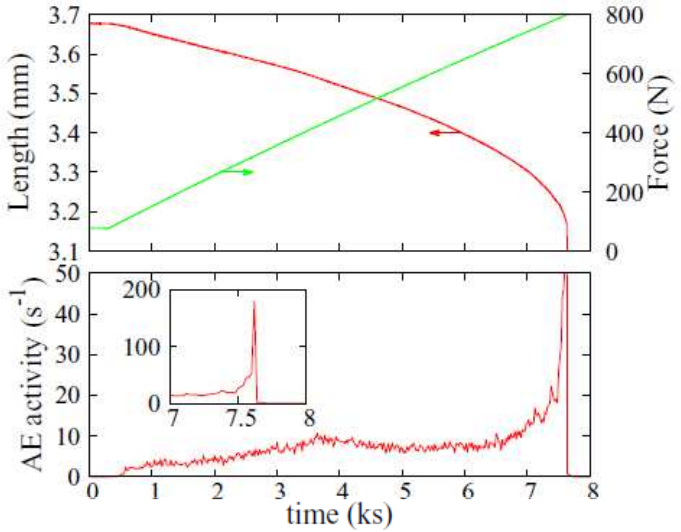

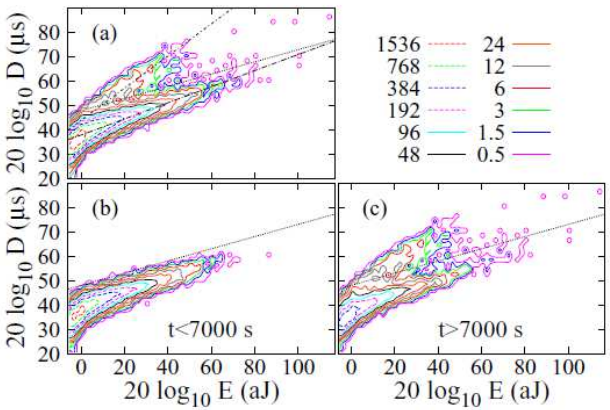

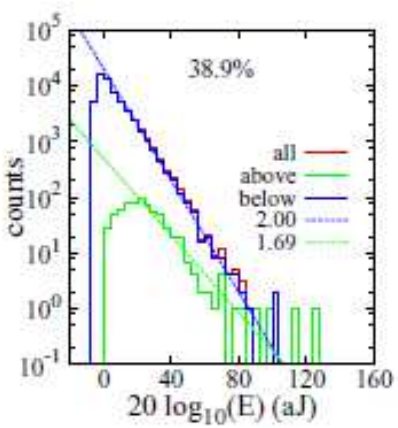

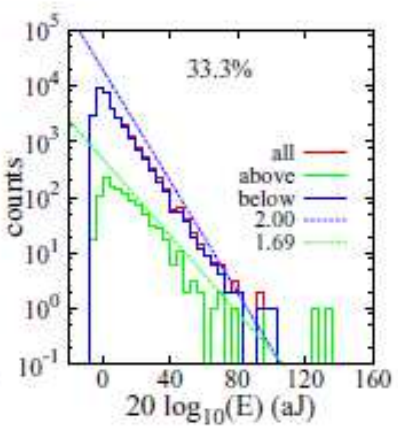

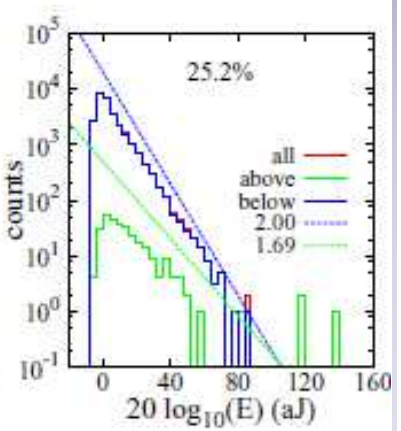

Soto-Parra et al., PRE, **91**, 060401(R) (2015)

Conclusions

- Acoustic emission provides information on the dynamical collective behaviour during the martensitic transformations.
- Avalanche criticality occurs in thermally and stress induced martensitic transformations after enough cycling across the transition.
- In MT, critical exponents depend essentially on symmetry change (variant multiplicity) at the transition and on the driving mechanism.
- In compressed porous materials acoustic emission can be analysed with the same statistical laws governing earthquakes.
- Critical exponents are very similar to those reported for earthquakes.
- The study of *labquakes* in compressed Vycor provides a laboratory experiment that can be used as a low-scale model for earthquakes with the final aim of predicting earthquake occurrence.
- In porous Ti-Ni under compression two families of signals can be identified, that show different criticalities.